NACA

RESEARCH MEMORANDUM

A TRANSONIC-WING INVESTIGATION IN THE LANGLEY 8-FOOT HIGH-SPEED TUNNEL AT HIGH SUBSONIC MACH NUMBERS AND AT A MACH NUMBER OF 1.2

WING-FUSELAGE CONFIGURATION HAVING A WING OF 0° SWEEPBACK, ASPECT RATIO 4.0, TAPER RATIO 0.6, AND NACA 65A006 AIRFOIL SECTION

By Maurice S. Cahn and Carroll R. Bryan

Langley Aeronautical Laboratory
Langley Field, Va.

NATIONAL ADVISORY COMMITTEE FOR AERONAUTICS

WASHINGTON
March 6, 1951

Classification cancelled (or changed to) Unclassified

By Authority of NASA Tech Pub Announcement #96

(OFFICER AUTHORIZED TO CHANGE)

By ..... 10 Feb 66

NK

..... GRADE OF OFFICER

7 Apr 67

DATE

NATIONAL ADVISORY COMMITTEE FOR AERONAUTICS

RESEARCH MEMORANDUM

A TRANSONIC-WING INVESTIGATION IN THE LANGLEY 8-FOOT HIGH-SPEED TUNNEL AT HIGH SUBSONIC MACH NUMBERS AND AT A MACH NUMBER OF 1.2

WING-FUSELAGE CONFIGURATION HAVING A WING OF 0° SWEEPBACK, ASPECT RATIO 4.0, TAPER RATIO 0.6, AND NACA 65A006 AIRFOIL SECTION

By Maurice S. Cahn and Carroll R. Bryan

SUMMARY

As part of an NACA transonic research program, a series of wing-body combinations is being tested in the Langley 8-foot high-speed tunnel. This paper presents the results of an investigation of a wing-fuselage combination utilizing a wing of unswept quarter-chord line, aspect ratio 4, taper ratio 0.6, and an NACA 65A006 airfoil section. Lift, drag, and pitching-moment characteristics, downwash angles, and wake losses for various angles of attack at high subsonic Mach numbers and at a Mach number of 1.2 are presented.

Increasing the free-stream Mach number at low lift coefficients caused the wing-fuselage configuration to exhibit a decrease in lift-curve slope beginning at a Mach number of 0.90, a rapid decrease in the maximum lift-drag ratio at a Mach number of 0.85, a rearward movement of the aerodynamic center at a Mach number of 0.87, and a shift in the angle of attack for zero downwash at a Mach number of 1.2. Also, at low lift coefficients, an increase of lift-curve slope and a rearward shift of the aerodynamic center with increasing lift coefficient were indicated at Mach numbers below 0.875. At high angles of attack, the wake 1.225 semispans behind the 25-percent mean-aerodynamic-chord station extended at least 0.375 semispan above the wing-chord plane.

INTRODUCTION

A general research program is being conducted by the National Advisory Committee for Aeronautics to supply designers of transonic aircraft with needed information on the effect of various wing-geometry parameters on aerodynamic characteristics at transonic speeds.

This paper presents the results of tests on a sting-supported wing-fuselage combination employing the unswept wing of a series of wings having varying amounts of sweep, aspect ratio 4, taper ratio 0.6, and an NACA 65A006 airfoil section. Tests on other wings in this series are reported in references 1, 2, and 3.

Lift, drag, and pitching-moment data are presented for subsonic Mach numbers from 0.60 to 0.93 and for a supersonic Mach number of 1.2. Also presented are point downwash data and wake losses for several tail heights at two spanwise locations.

The data presented herein and in references 1, 2, and 3 are compared with data of geometrically similar configurations obtained by means of the transonic-bump method in the Langley 7- by 10-foot tunnel (see reference 4).

SYMBOLS

C_D	drag coefficient $\left(\frac{D}{qS}\right)$
C_L	lift coefficient $\left(\frac{L}{qS}\right)$
C_m	pitching-moment coefficient referred to $0.25\bar{c}$ $\left(\frac{M_{\bar{c}/4}}{qS\bar{c}}\right)$
$\bar{c}$	mean aerodynamic chord, inches
D	drag, pounds
ΔH	loss of total pressure in wake, pounds per square foot
ΔP	pressure difference between upper and lower components of a yaw tube
L	lift, pounds
M	Mach number

$M_{\bar{c}/4}$	pitching moment about 25 percent $\bar{c}$, inch-pounds
P_b	base-pressure coefficient $\left(\frac{p_b - p_o}{q}\right)$
p_o	free-stream static pressure, pounds per square foot
p_b	static pressure at model base, pounds per square foot
q	free-stream dynamic pressure, pounds per square foot $\left(\frac{1}{2}\rho V^2\right)$
q_L	local dynamic pressure at any yaw tube
R	Reynolds number based on $\bar{c}$
S	wing area of model, square feet
V	free-stream velocity, feet per second
α	angle of attack of fuselage center line, degrees
ϵ	downwash angle, degrees
ρ	free-stream density, slugs per cubic foot

APPARATUS AND METHODS

Tunnel

The investigation was conducted in the Langley 8-foot high-speed tunnel, utilizing the plaster-lined nozzle described in reference 5. Subsonic tests were conducted with the model located in the region of the minimum section of the nozzle. For testing at a Mach number of 1.2, the model was moved downstream to the expanded section of the nozzle.

The minimum section of the nozzle had a constant Mach number distribution up to the highest point tested. In the supersonic section of the nozzle, the maximum Mach number variation was 0.02.

Model and Support

The model tested had a wing with 0° sweepback of the quarter-chord line, zero twist and dihedral, aspect ratio of 4, taper ratio of 0.6, and an NACA 65A006 airfoil section measured parallel to the model plane of

symmetry. The wing was machined from 14ST aluminum alloy, and was mounted on a fuselage body of revolution of fineness ratio 10.0. The longitudinal position of the wing was such that the quarter-chord point of the mean aerodynamic chord coincided with the station of maximum body diameter. Principal wing dimensions are presented with a plan-form drawing of the wing-fuselage combination in figure 1. The fuselage ordinates and dimensions are presented in figure 2. An electrical strain-gage balance was contained within the fuselage and secured to the fuselage at the forward end. The rear part of the balance comprised a sting for supporting the model in the center of the tunnel (reference 1). The sting was hinged to a support tube in such a manner that the angle of attack could be varied by means of a remote-control mechanism while testing was in progress. This sting-support tube could be made to slide axially on its mounts in order to move the model from the subsonic test section to the supersonic test section. Figure 3 is a diagram of this setup and figure 4 gives a general view of the model, sting, sting support, and test section.

Measurements

Lift, drag, and pitching-moment data were obtained by using the internal-strain-gage-balance system. The sensitivity of the strain-gage balance and the scatter of test points indicated that the accuracy of lift, drag, and pitching-moment coefficients was within ±0.01, ±0.001, and ±0.005, respectively, for all Mach numbers. Downwash and wake-intensity measurements were made with two rakes having both yaw-pressure and total-pressure tubes. The location and geometry of these rakes are shown in figure 5. Angles of attack of the model and of the rake were determined within 0.1° by means of an optical system utilizing parallel light beams. A description of this device can be found in reference 1. A photograph of the model and rake setup is shown in figure 6. The static pressure at the base of the model was determined by means of a static orifice located on the side of the sting in the plane of the model base.

The yaw tubes were calibrated in the empty test section by measuring the variation of $\frac{\Delta P}{q_L}$ with rake angle of attack. Downwash angles were determined with this calibration from the $\frac{\Delta P}{q_L}$'s measured during the tests. During these measurements the static pressure in the wake was assumed to be equal to the free-stream static pressure. Where the wake was large, this is a possible source of error; however, consideration of possible small errors in calibration, angle-of-attack measurements, scatter of tests points, and variations in local static pressure indicated the accuracy of the measured downwash angles to be within $\pm 0.2^\circ$ for measurements made outside the wake and within $\pm 0.3^\circ$ for measurements made in the wake.

Test Conditions

Data were taken at angles of attack of -2° through 14° at Mach numbers of 0.60 to 0.93 and at a Mach number of 1.2 for the wing-fuselage combination. Also, the wing-fuselage combination was tested at various Mach numbers in the above range with transition from laminar to turbulent boundary layer fixed at the 10-percent-chord line on the upper and lower surfaces of the wing and 4 inches back of the nose on the fuselage by means of number 60 carborundum grains doped to the model surface at these positions.

The variation of mean test Reynolds number with Mach number is shown in figure 7. Variations in atmospheric conditions caused deviations from this curve, but, for any given Mach number the Reynolds number did not differ from that shown by more than 3.5 percent.

By means of pressure measurements obtained from a series of static-pressure wall orifices, choking tendencies were observed in the tunnel. No data are presented in this report where these tendencies were evidenced.

At a Mach number of 1.2, the location of the normal shock was ascertained by means of a portable point light source. In none of the tests for which data are presented did the normal shock advance upstream ahead of the rakes or to the base of the model. This condition has been shown in reference 6 to be the criteria for effects of the normal shock on the model.

CORRECTIONS

Corrections due to tunnel-induced upwash and due to model and wake blockage and pressure gradient due to wake were calculated and applied to the data by using the methods of references 7, 8, and 9. The corrections to the dynamic pressure and to the Mach number were found to be negligible below a Mach number of 0.85 and reached a maximum of 1.4 percent at a Mach number of 0.93. The maximum correction to the downwash angle at the rakes amounted to 0.2°.

Base-pressure coefficients were obtained and are presented in figure 8. Comparison of these base pressures with the base pressures from reference 1 for the fuselage-alone configuration indicated that the addition of the wing lowered the base-pressure coefficient by an amount approaching 100 percent at the higher angles of attack.

No tare corrections have been applied except in the case of sting tare; for this case, the corrections were applied to the maximum

lift-to-drag ratio and to drag at zero lift. The results of the investigation of a similar model at low angles of attack (reference 10) indicated that this tare need not be applied to lift or moment values but would be an increment of 0.003 to be added to the drag coefficient at all subsonic Mach numbers and 0.002 at a Mach number of 1.2. As the test setup in reference 10 involved a sting-support system similar to the support system in the present test, corresponding sting corrections in the two tests are assumed to be of the same order of magnitude. It is also estimated that the sting may cause the downwash angles to be decreased by as much as 1° at subsonic Mach numbers and 0.1° at a Mach number of 1.2. In addition, the base-pressure coefficients may be increased by the presence of the sting by approximately 0.1 at all Mach numbers. Inasmuch as these corrections were estimated by using data from reference 10, which only consider low angles of attack, no attempt has been made to apply them to the data except in the aforementioned cases.

Corrections in the angle of attack due to the sweep of the center-of-bending line and due to a pitching moment on the wing were calculated and found to be of negligible value.

RESULTS AND DISCUSSION

In this investigation, a wing-fuselage combination was tested as the basic configuration. Fuselage-alone data were subtracted from the data of the wing-fuselage combination and the resulting data are the wing-with-wing-fuselage-interference data. Basic data for the fuselage alone may be found in reference 1.

All of the following discussion pertains to transition-natural data unless otherwise stated.

A table of figures presenting the results follows:

	Figure
Wing-fuselage force data against Mach number	9
Wing-fuselage force data against lift coefficient	10
Wing-with-wing-fuselage-interference force data against lift coefficient	11
Lift-curve slope against Mach number	12
Zero-lift drag coefficient against Mach number	13
Maximum lift-drag ratio against Mach number	14
Static-longitudinal-stability parameter against Mach number	15
Wake losses (wing-fuselage)	16
Point downwash data against angle of attack	17
Average rate of change of downwash angle with angle of attack against Mach number	18

Force and Moment Characteristics

The decrease in lift coefficient for the wing-fuselage configuration occurred at a Mach number of approximately 0.90 for angles up to 4° (fig. 9(a)). Fixing transition caused a reduction in lift coefficient at the high Mach numbers for angles of attack up to 10°.

At a Mach number of 0.60, the lift-curve slope for the wing-fuselage configuration was 0.068 at zero lift (fig. 12). The slope then increased to a maximum of 0.104 at a Mach number of 0.90. At a Mach number of 1.2, the slope was 0.08. The lift-curve slope at a lift coefficient of 0.4 had the same trends. The magnitude, however, was approximately 12 percent higher at a Mach number of 0.60 and reached its peak value of 0.107 at a Mach number of 0.85. At a Mach number of 1.2, the lift-curve slope at a lift coefficient of 0.4 was 11 percent lower than the lift-curve slope at zero lift coefficient. It is suspected that the increase in lift-curve slope with increasing lift coefficient at the lower speeds was associated with a separation bubble similar to that described in reference 11. This flow characteristic, however, decreases with increasing Reynolds number and would probably disappear at a Reynolds number of approximately 10 million. A decrease in lift-curve slope at the high lift coefficients occurs when the separated region extends over a large part of the chord.

Subtracting the fuselage data from the wing-fuselage data had little effect on the lift-curve slopes except at a lift coefficient of 0.4 where the peak was reduced by 5 percent.

At low lift coefficients, an abrupt drag rise occurred at a Mach number of approximately 0.875 (fig. 9(b)). In general, fixing transition resulted in an increase in drag coefficient, but in no instance did the transition-fixed data show any marked drag changes over the natural-transition data.

At zero lift, the drag coefficient for the wing-fuselage combination remained constant at approximately 0.009 up to a Mach number of 0.875, where it increased sharply (fig. 13). At a Mach number of 1.2, this drag coefficient was 0.038. The same trends for zero lift drag were exhibited by the wing-with-wing-fuselage-interference data. However, the absolute values of this coefficient were approximately 72 percent lower at subsonic speeds and approximately 26 percent lower at a Mach number of 1.2 than the corresponding values for the wing-fuselage configuration.

A maximum lift-to-drag ratio of approximately 14.5 for the wing-fuselage combination was maintained up to a Mach number of 0.85 (fig. 14). Above this Mach number, a rapid decrease in lift-to-drag ratio was caused by an abrupt drag rise. At a Mach number of 1.2, this ratio

was 5.5. The lift-to-drag ratio for the wing-with-wing-fuselage-interference data was approximately 73 percent higher than that for the wing-fuselage configuration up to a Mach number of 0.85, above which the increase was much less pronounced. At a Mach number of 1.2, this increase was only 22 percent.

The large favorable changes in drag at zero lift and in maximum lift-to-drag ratios resulting from subtracting the fuselage data from the wing-fuselage data are largely due to the fact that the drag of the part of the wing covered by the fuselage does not appear in the resulting configuration, although the coefficients are based on the total area of the wing.

The wing-fuselage configuration exhibited an abrupt decrease in pitching-moment coefficient beginning at a Mach number of 0.86 for 2° angle of attack and at lower Mach numbers for higher angles of attack. Fixing transition reduced the abruptness and magnitude of this variation. At zero lift, the longitudinal stability parameter $\frac{\partial C_m}{\partial C_L}$ remained at a constant value of 0.15 up to a Mach number of 0.85 (fig. 15). Above 0.85 the aerodynamic center began to move rearward, the model becoming neutrally stable at a Mach number of 0.905. At a Mach number of 1.2, the moment-curve slope indicated stability, being -0.09. At a lift coefficient of 0.4, the aerodynamic center at subsonic speeds was approximately 5 percent rearward of the location for zero lift. This rearward shift with increasing angle of attack may be associated with the leading-edge separation previously mentioned. For a lift coefficient of 0.4, the aerodynamic center began a rapid rearward movement at a Mach number of 0.80. This rearward movement resulted in the wing-fuselage configuration becoming stable above a Mach number of 0.85 where the value of $\frac{\partial C_m}{\partial C_L}$ reached -0.08. At a Mach number of 1.2, the slope of the moment curve was essentially the same for a lift coefficient of 0.4 as it was for zero lift.

For both lift coefficients, subtracting the fuselage-alone moment moved the aerodynamic center rearward approximately 7 percent of the mean aerodynamic chord at most speeds.

Wake and Downwash Characteristics

At Mach numbers of 0.6 and 0.8, the wake losses for 0° and 4° were negligible in the region investigated, but, at a Mach number of 0.93, the wake for 4° had begun to appear; thus a shock-induced separation was indicated (fig. 16). At a Mach number of 1.2, the shock had moved to the trailing edge, and wake losses were again small for 0° and 4°.

The wake for 10° was assumed to extend at least 0.375 semispan above the fuselage at all speeds tested. The wake losses at the inboard station were larger than those of the outboard station because of losses due to the fuselage.

A significant change in the angle of attack for zero downwash occurred at a Mach number of 1.2 (fig. 17) for the wing-fuselage combination as compared with this configuration at a Mach number of 0.93. As a consequence, significant changes in trim of an airplane flying to a Mach number of 1.2 can be expected from this shift if the horizontal tail is located within the region investigated. This shift in the angle of attack for zero downwash is attributed to the fuselage inasmuch as wing-with-wing-fuselage-interference data did not indicate a similar change.

The average rate of change of downwash angle with angle of attack is presented against Mach number in figure 18. These values were found by averaging the slopes for the two semispan stations at a location 0.375 semispan above the wing-chord plane. This average $\frac{\partial \epsilon}{\partial \alpha}$ for the wing-fuselage combination at a Mach number of 0.80 was approximately 0.5 and 0.6 for lift coefficients of 0 and 0.4, respectively. Wing-with-wing-fuselage-interference data below a Mach number of 0.80 exhibited a zero lift $\frac{\partial \epsilon}{\partial \alpha}$ approximately 12 percent lower and a $\frac{\partial \epsilon}{\partial \alpha}$ for a lift coefficient of 0.4 approximately 15 percent higher than corresponding values for the wing-fuselage configuration. Variation of $\frac{\partial \epsilon}{\partial \alpha}$ with Mach number was erratic above a Mach number of 0.80.

CONCLUSIONS

The results of an investigation of a wing-fuselage combination employing a wing with unswept quarter-chord line, aspect ratio 4, taper ratio 0.6, and an NACA 65A006 airfoil section at high subsonic Mach numbers and at a Mach number of 1.2 indicated the following:

1. Increasing the free stream Mach number at low lift coefficients caused the wing-fuselage configuration to exhibit a decrease in lift-curve slope at a Mach number of 0.90, a rapid decrease in the maximum lift-to-drag ratio at a Mach number of 0.85, and a rearward movement of the aerodynamic center at a Mach number of 0.87.

2. An increase in lift-curve slope and rearward shift of aerodynamic center with increasing angle of attack was indicated at low Mach numbers.

3. The wake 1.225 semispans behind the 25-percent mean-aerodynamic-chord station extended to at least 0.375 semispan above the wing-chord plane at high angles of attack.

4. At a Mach number of 1.2, the angle of attack for zero downwash was changed by the presence of the fuselage; thus significant changes in trim going from a Mach number of 0.93 to a Mach number of 1.2 occurred.

Langley Aeronautical Laboratory
National Advisory Committee for Aeronautics
Langley Field, Va.

REFERENCES

1. Osborne, Robert S.: A Transonic-Wing Investigation in the Langley 8-Foot High-Speed Tunnel at High Subsonic Mach Numbers and at a Mach Number of 1.2. Wing-Fuselage Configuration Having a Wing of 45° Sweepback, Aspect Ratio 4.0, Taper Ratio 0.6, and NACA 65A006 Airfoil Section. NACA RM L50H08, 1950.

2. Henry, Beverly Z., Jr.: A Transonic-Wing Investigation in the Langley 8-Foot High-Speed Tunnel at High Subsonic Mach Numbers and at a Mach Number of 1.2. Wing-Fuselage Configuration Having a Wing of 35° Sweepback, Aspect Ratio 4.0, Taper Ratio 0.6, and NACA 65A006 Airfoil Section. NACA RM L50J09, 1950.

3. Wood, Raymond B. and Fleming, Frank F.: A Transonic-Wing Investigation in the Langley 8-Foot High-Speed Tunnel at High Subsonic Mach Numbers and at a Mach Number of 1.2. Wing-Fuselage Configuration Having a Wing of 60° Sweepback, Aspect Ratio 4.0, Taper Ratio 0.6, and NACA 65A006 Airfoil Section. NACA RM L50J25, 1951.

4. Donlan, Charles J., Myers, Boyd C., II, and Mattson, Axel T.: A Comparison of the Aerodynamic Characteristics at Transonic Speeds of Four Wing-Fuselage Configurations as Determined from Different Test Techniques. NACA RM L50H02, 1950.

5. Ritchie, Virgil S., Wright, Ray H., and Tulin, Marshall P.: An 8-Foot Axisymmetrical Fixed Nozzle for Subsonic Mach Numbers up to 0.99 and for a Supersonic Mach Number of 1.2. NACA RM L50A03a, 1950.

6. Ritchie, Virgil S.: Effects of Certain Flow Nonuniformities on Lift, Drag, and Pitching Moment for a Transonic Airplane Model Investigated at a Mach Number of 1.2 in a Nozzle of Circular Cross Section. NACA RM L9E20a, 1949.

7. Eisenstadt, Bertram J.: Boundary-Induced Upwash for Yawed and Swept-back Wings in Closed Circular Wind Tunnels. NACA TN 1265, 1947.

8. Goldstein, S., and Young, A. D.: The Linear Perturbation Theory of Compressible Flow, with Applications to Wind-Tunnel Interference. R. & M. No. 1909, A.R.C., 1943.

9. Herriot, John G.: Blockage Corrections for Three-Dimensional-Flow Closed-Throat Wind Tunnels, with Consideration of the Effect of Compressibility. NACA RM A7B28, 1947.

10. Osborne, Robert S.: High-Speed Wind-Tunnel Investigation of the Longitudinal Stability and Control Characteristics of a $\frac{1}{16}$-Scale Model of the D-558-2 Research Airplane at High Subsonic Mach Numbers and at a Mach Number of 1.2. NACA RM L9C04, 1949.

11. Nuber, Robert J., and Gottlieb, Stanley M.: Two-Dimensional Wind-Tunnel Investigation at High Reynolds Numbers of an NACA 65A006 Airfoil with High-Lift Devices. NACA RM L7K06, 1948.

WING DIMENSIONS

Airfoil section (parallel to model plane of symmetry - NACA 65A006	
Area, sq ft	1
Aspect ratio	4
Taper ratio	0.6
Sweep angle, deg (25-percent chord line	0
Incidence, deg	0
Dihedral, deg	0
Geometric twist, deg	0

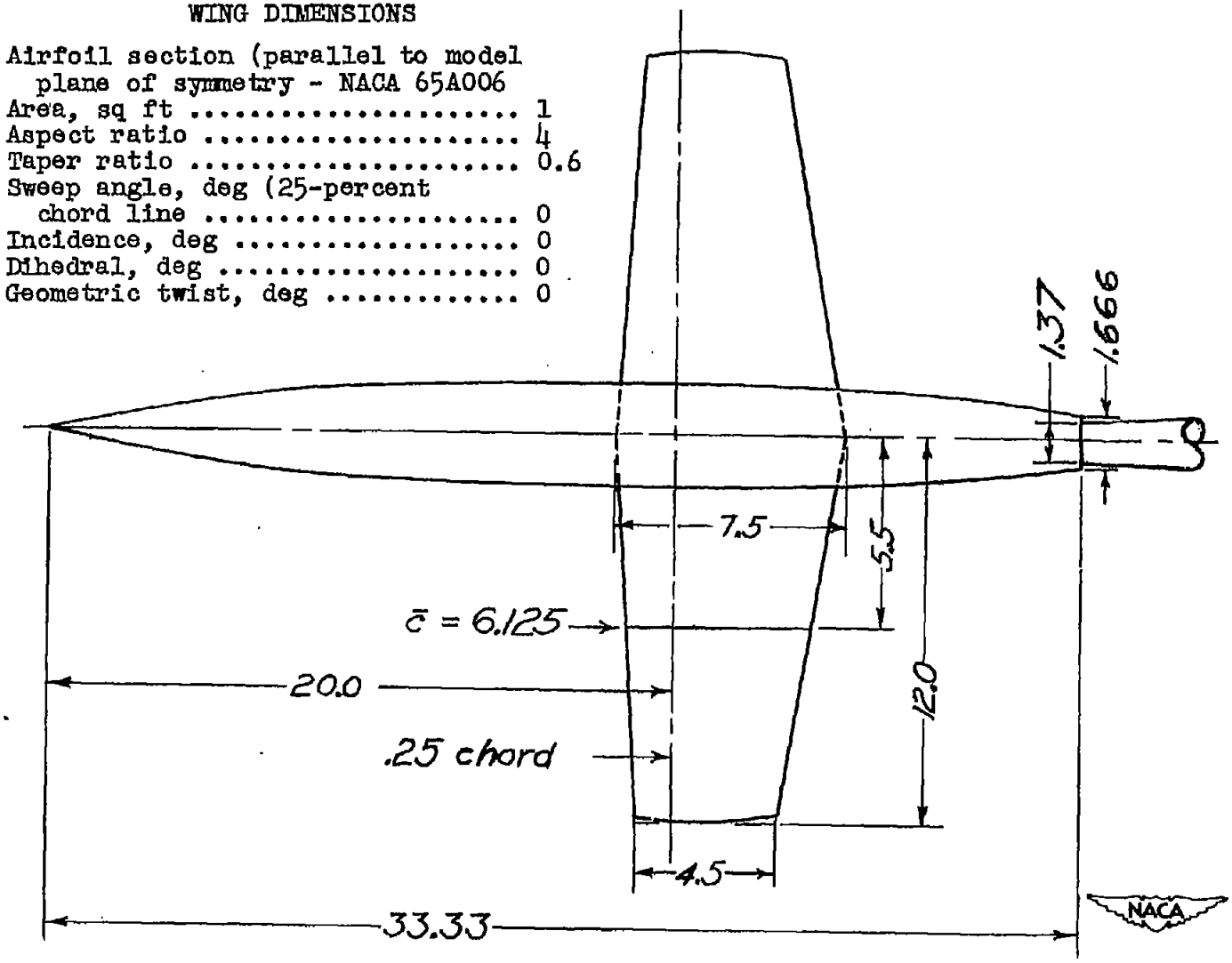

Figure 1.- Plan view of model giving over-all dimensions. All dimensions are in inches.

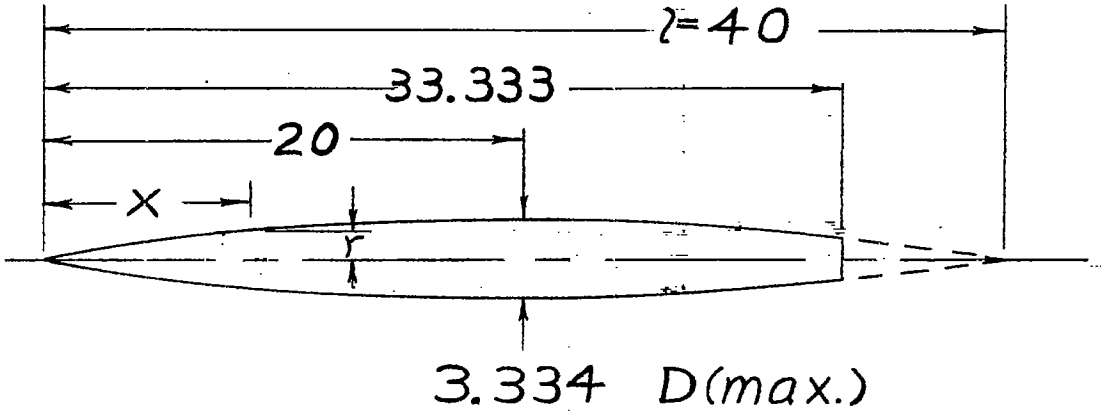

ORDINATES			
x/l	r/l	x/l	r/l
0	0		
.0050	.00231	.4500	.04143
.0075	.00298	.5000	.04167
.0125	.00428	.5500	.04130
.0250	.00722	.6000	.04024
.0500	.01205	.6500	.03842
.0750	.01613	.7000	.03562
.1000	.01971	.7500	.03128
.1500	.02593	.8000	.02526
.2000	.03090	.8333	.02083
.2500	.03465	.8500	.01852
.3000	.03741	.9000	.01125
.3500	.03933	.9500	.00439
.4000	.04063	1.0000	0
L.E. radius = 0.0005l			

Fineness ratio 10
$\bar{c}/4$ located at D(max.)

Figure 2.- Fuselage details. All dimensions are in inches.

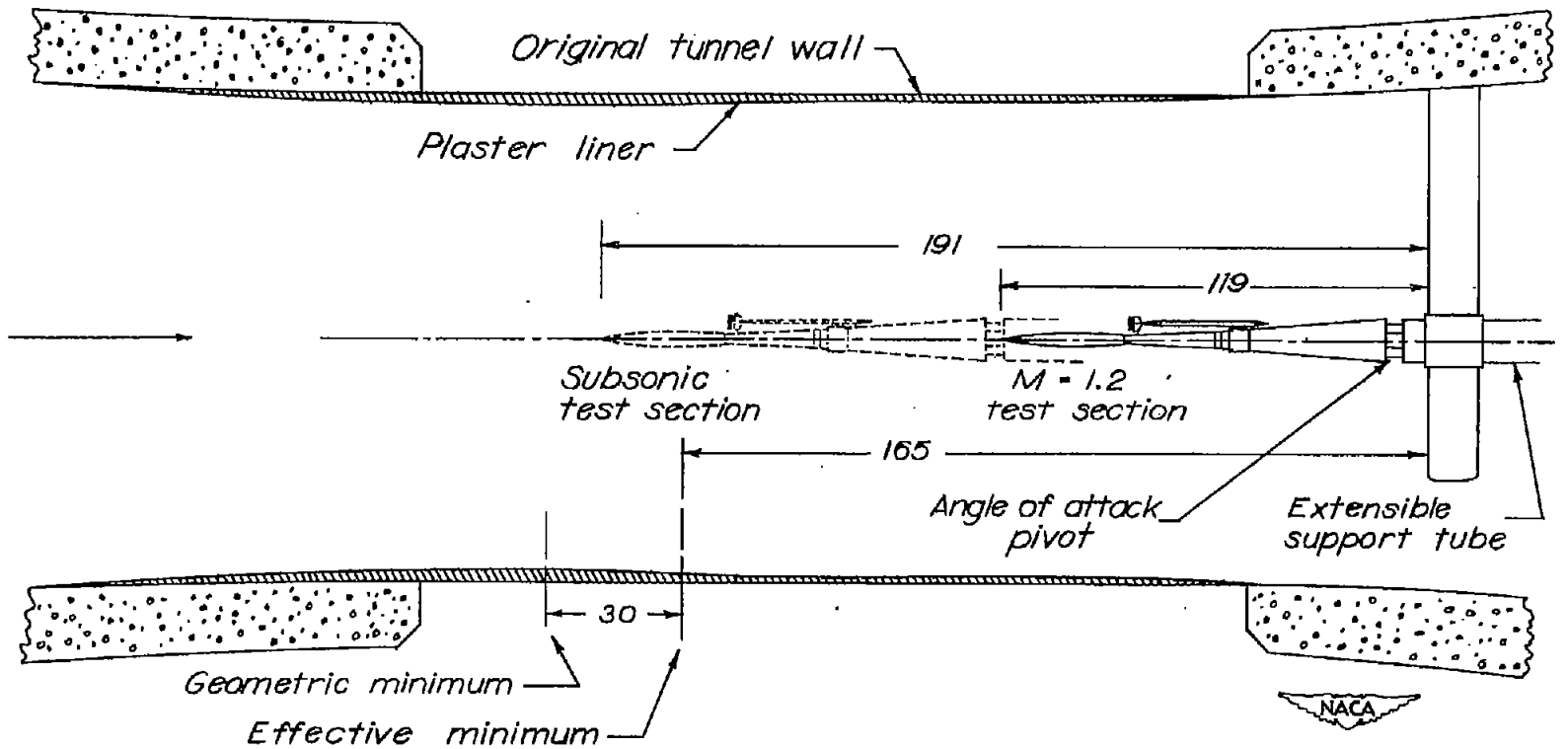

Figure 3.- Location of model in relation to Langley 8-foot high-speed-tunnel test section and support system.

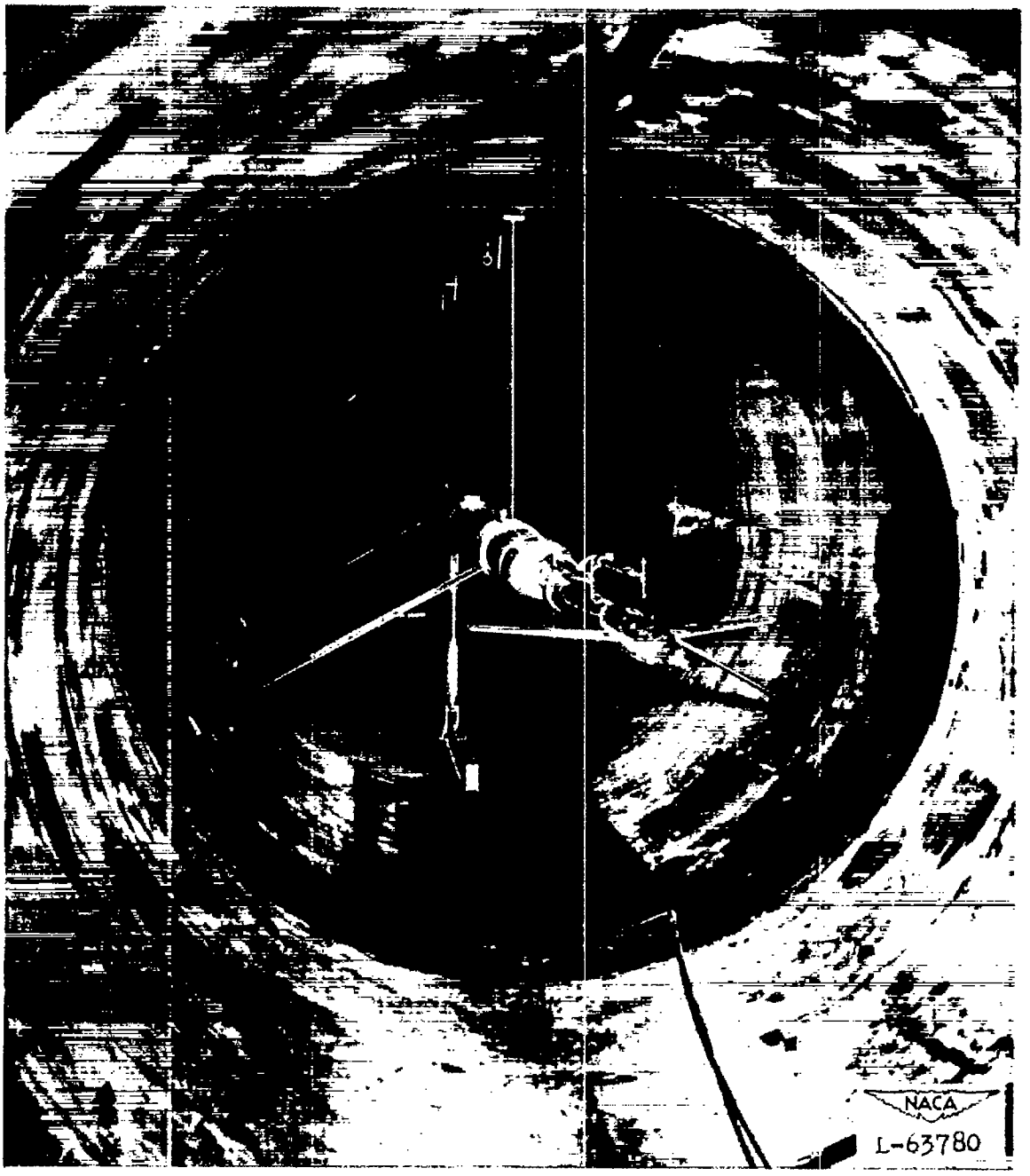

Figure 4.- General view of test setup showing model, rakes, and support system.

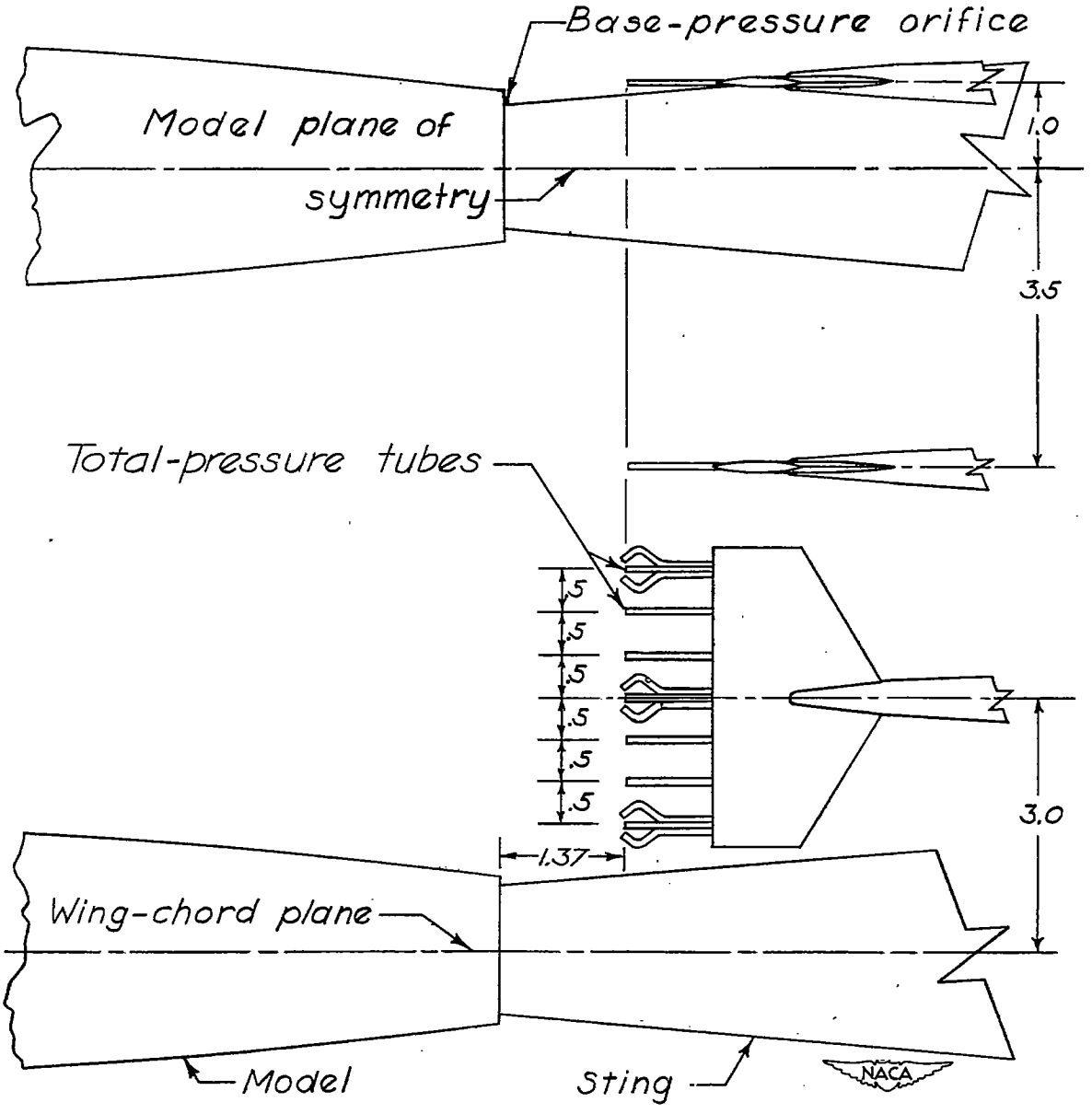

Figure 5.- Details of the rakes used for wake survey and downwash measurement. All dimensions are in inches.

Figure 6.- Photograph of model as tested in the Langley 8-foot high-speed tunnel.

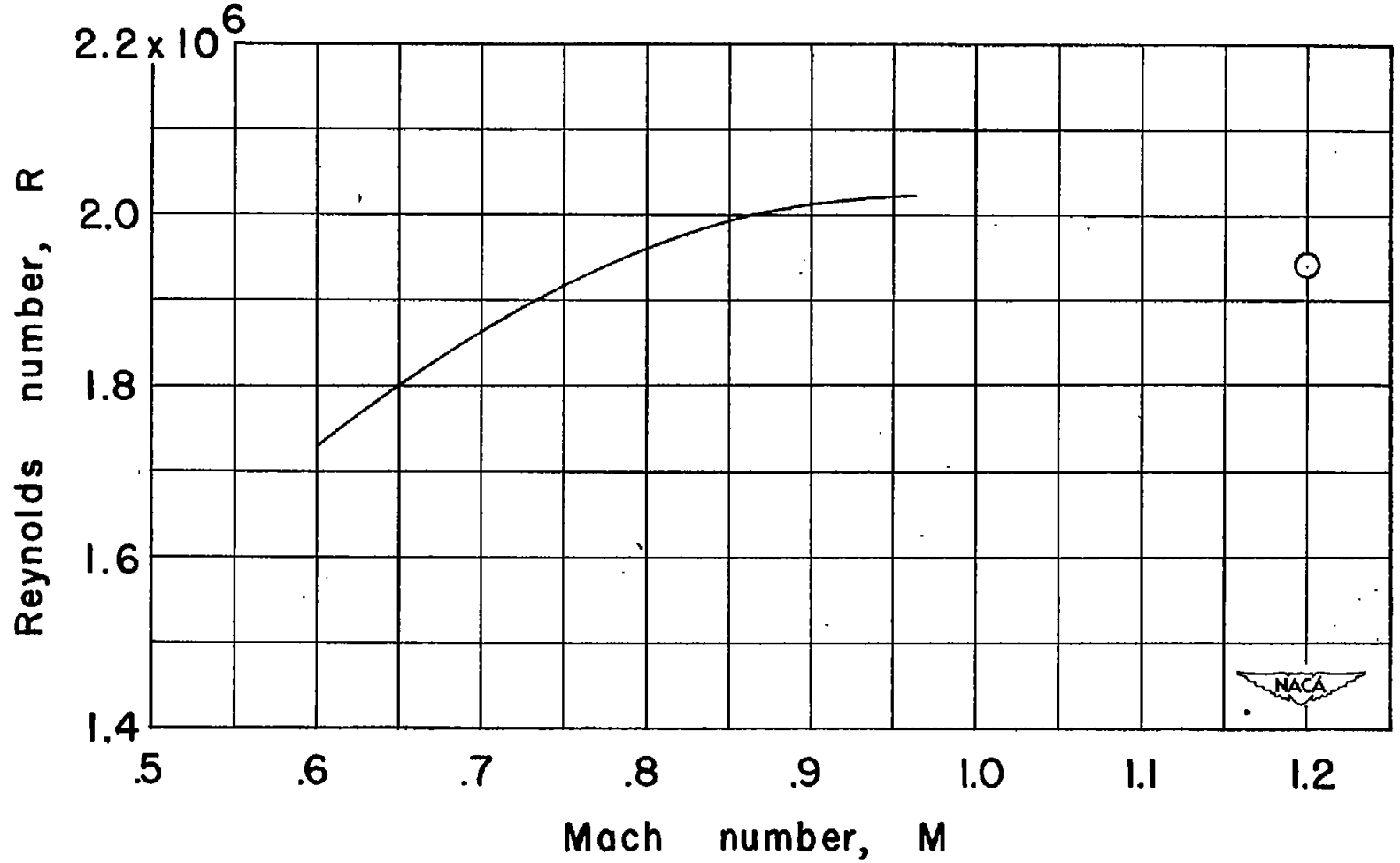

Figure 7.- Variation of test Reynolds number based on a $\bar{c}$ of 6.125 inches, with Mach number.

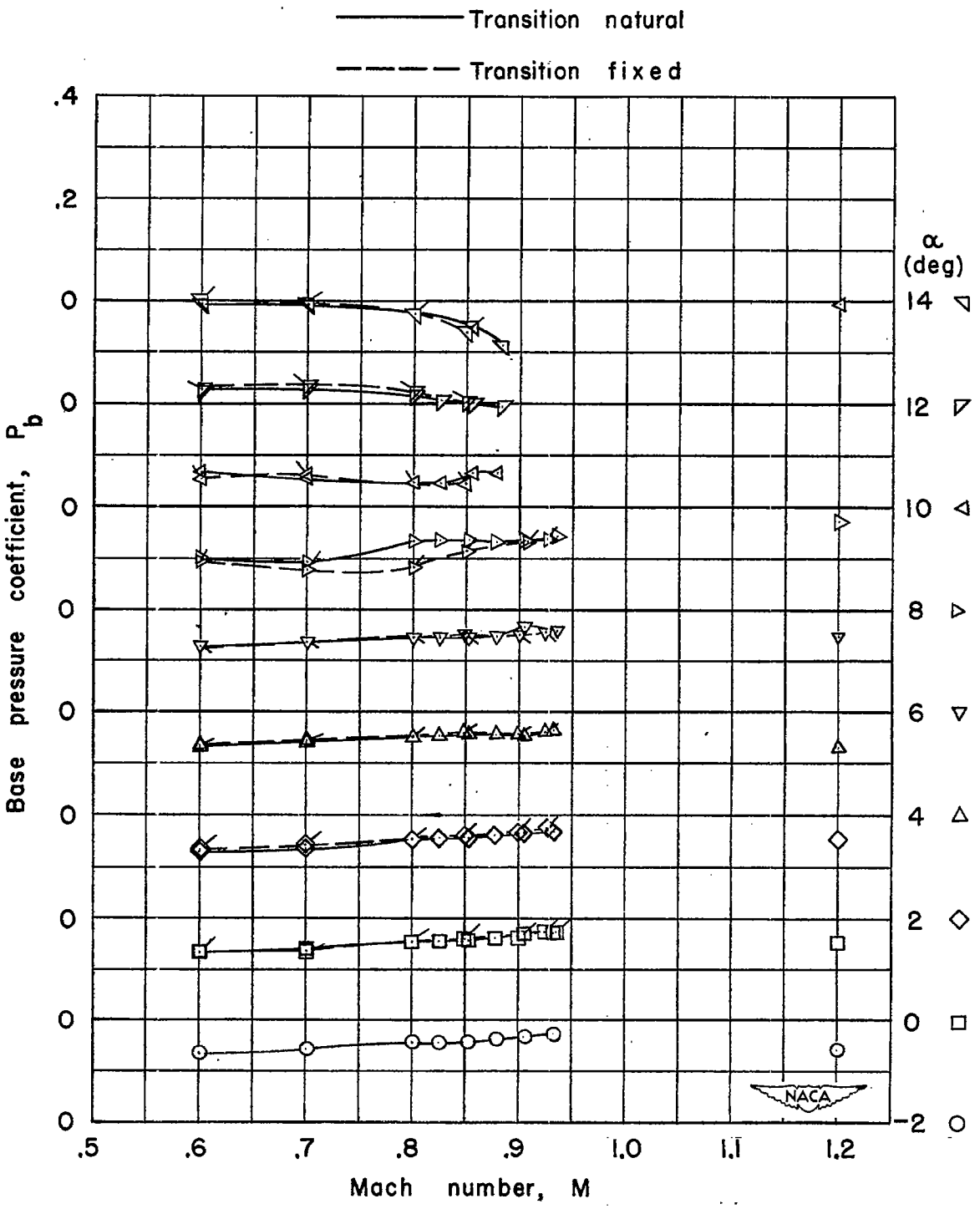

Figure 8.- Base-pressure-coefficient variation with Mach number. Unflagged symbols indicate transition natural.

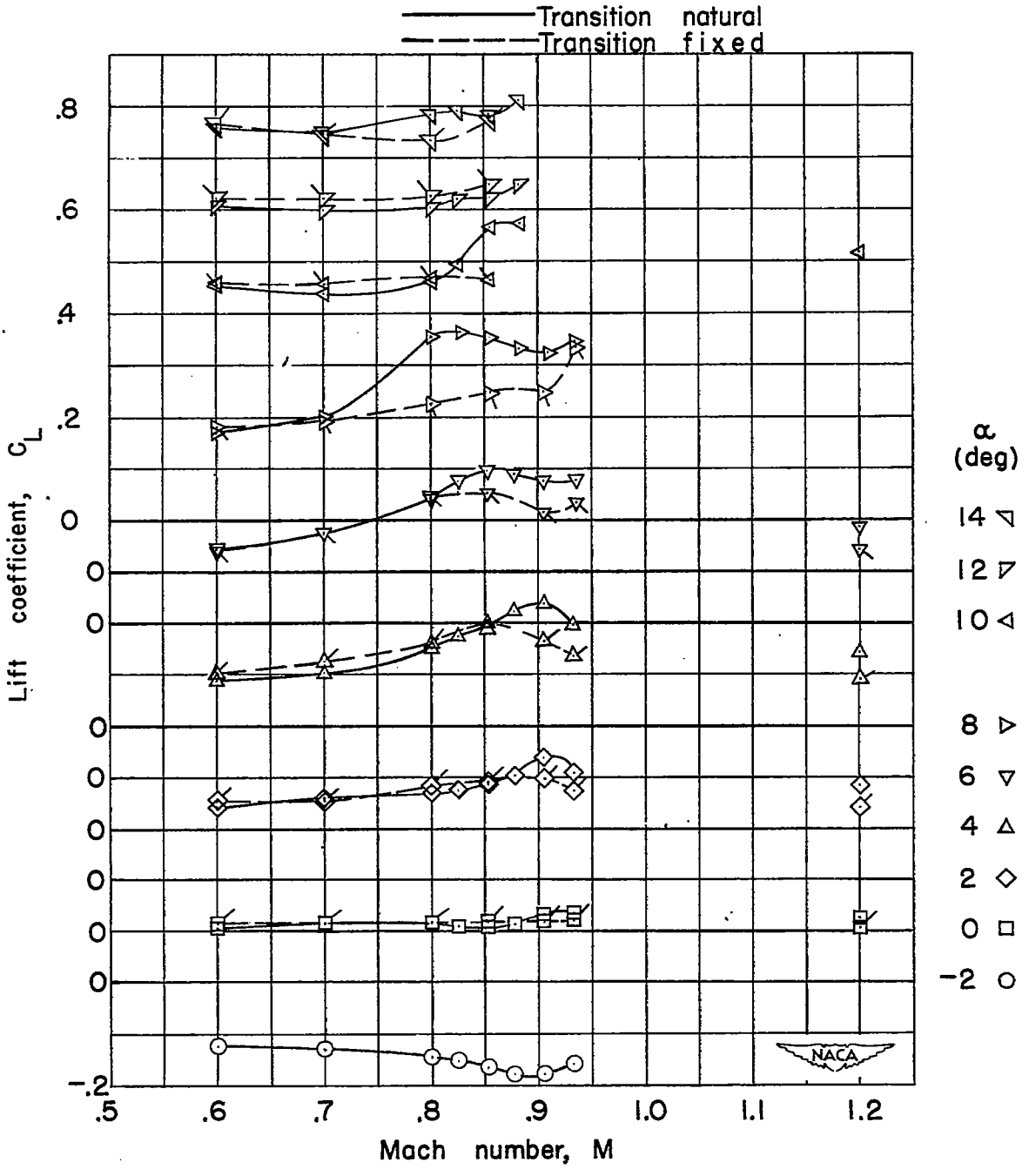

(a) Lift coefficient.

Figure 9.- Variation with Mach number of the aerodynamic coefficients of the wing-fuselage configuration with transition natural and with transition fixed on the 10-percent-chord line of the wing. Unflagged symbols indicate transition natural.

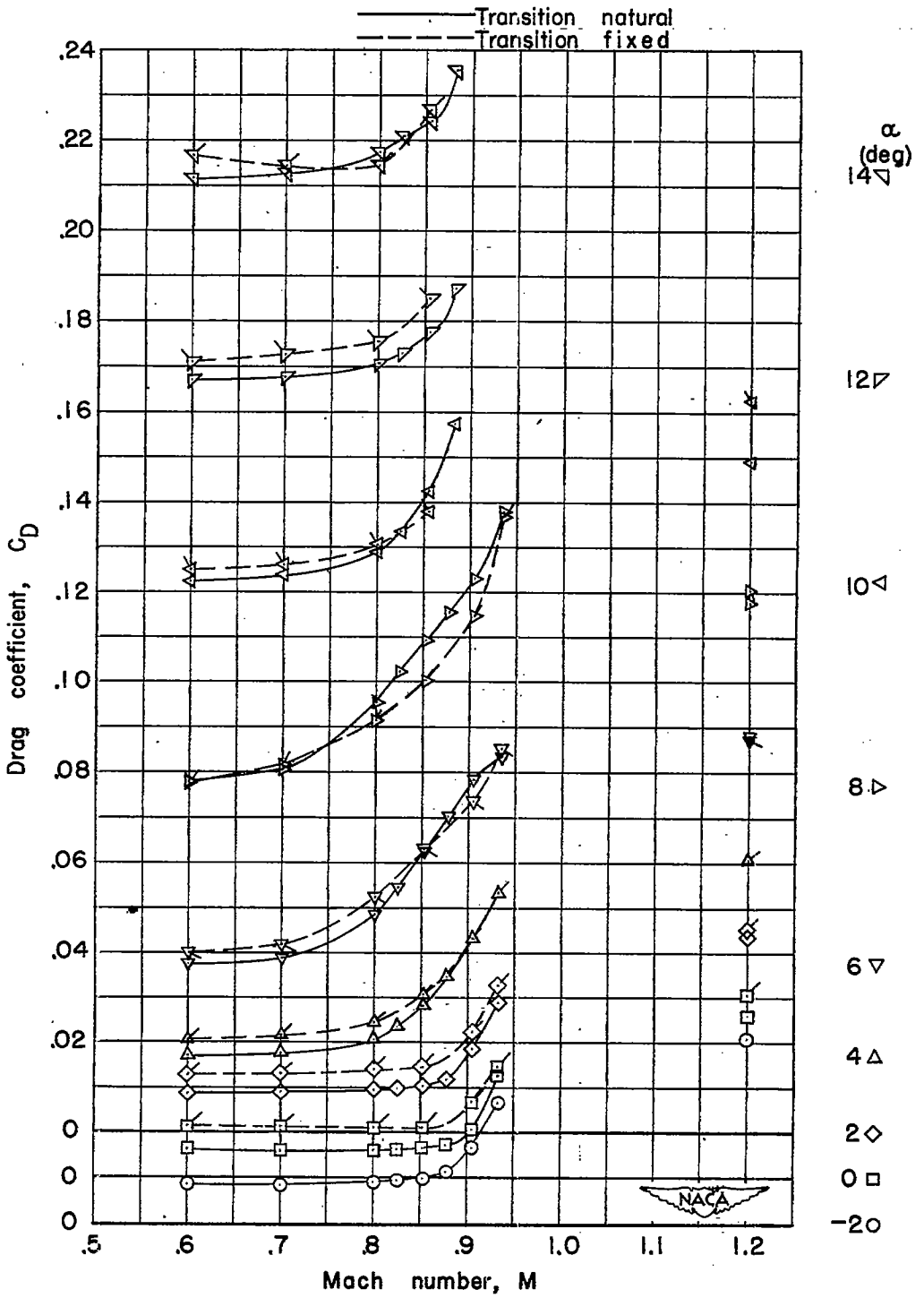

(b) Drag coefficient.

Figure 9.- Continued.

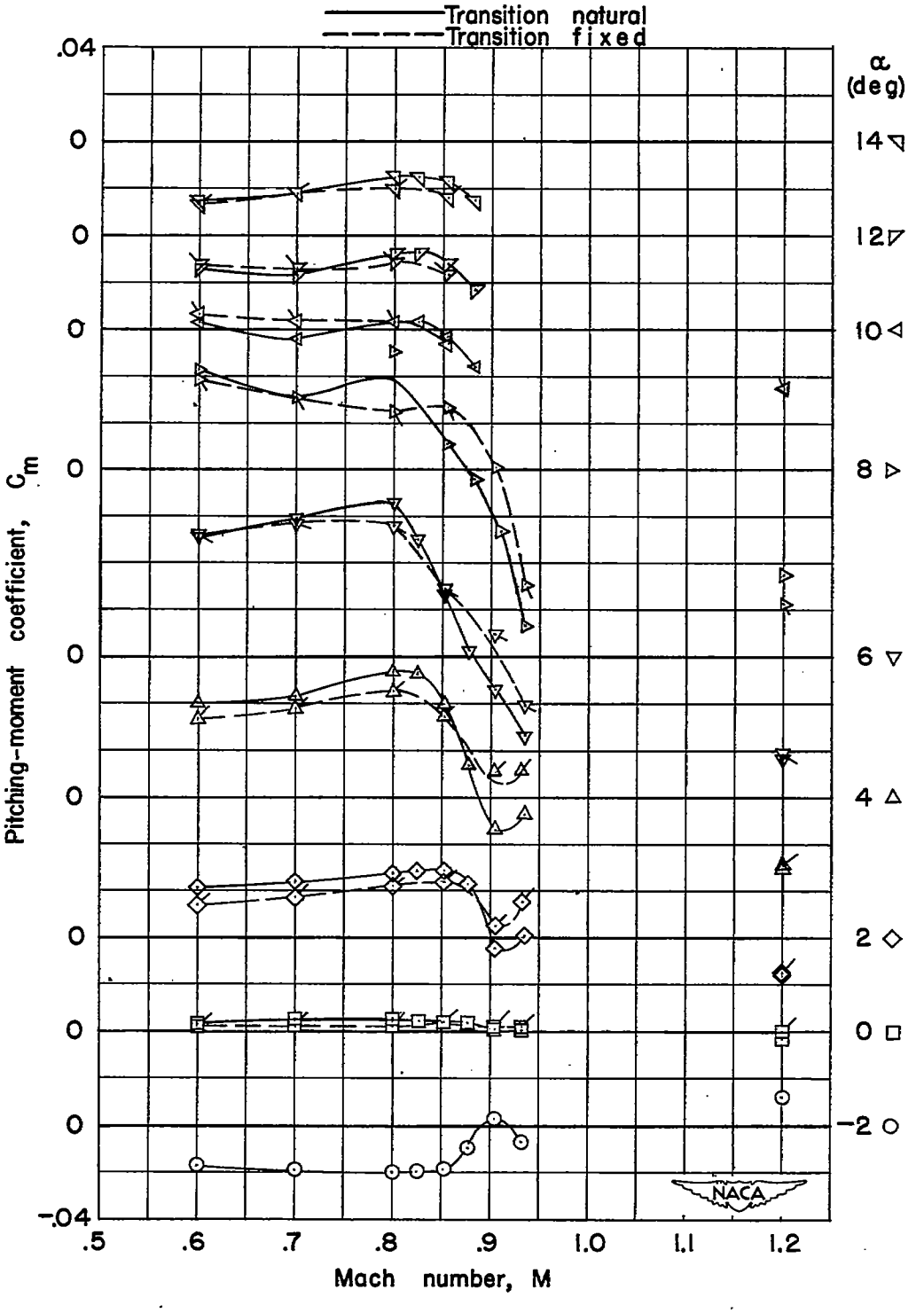

(c) Pitching-moment coefficient.

Figure 9.- Concluded.

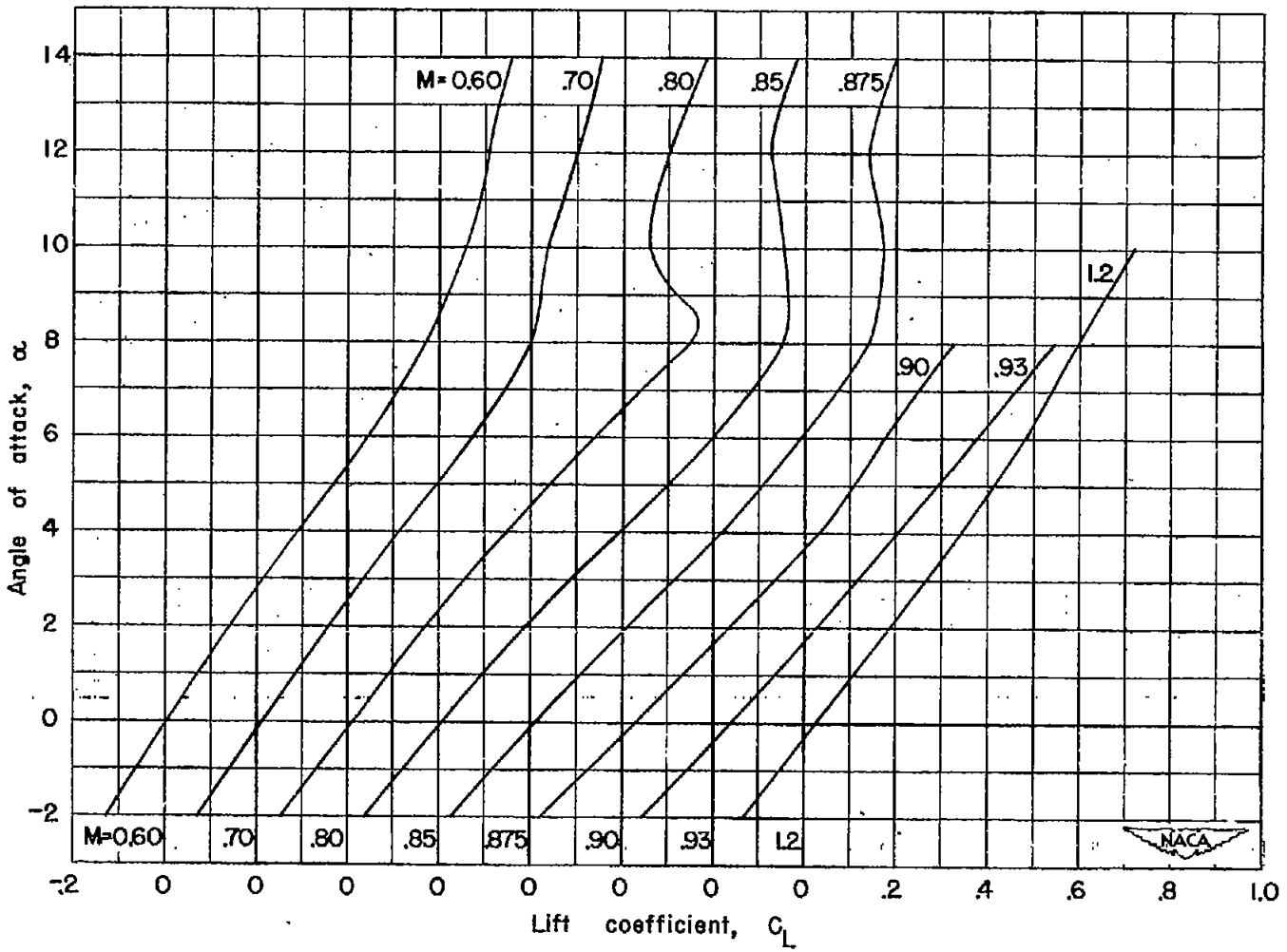

(a) Angle of attack.

Figure 10.- Variation of the aerodynamic coefficients with lift coefficient for the wing-fuselage configuration.

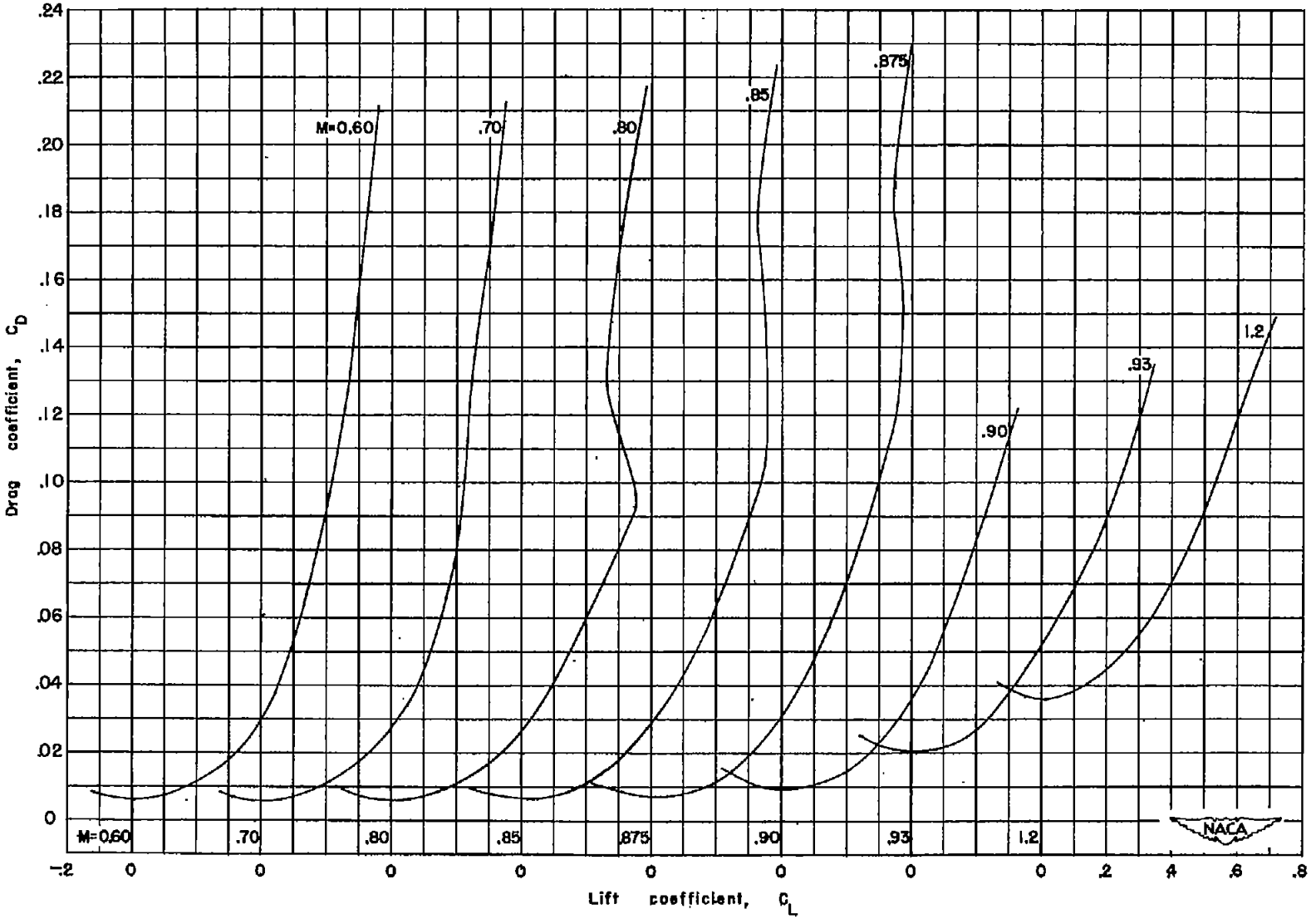

(b) Drag coefficient.

Figure 10.- Continued.

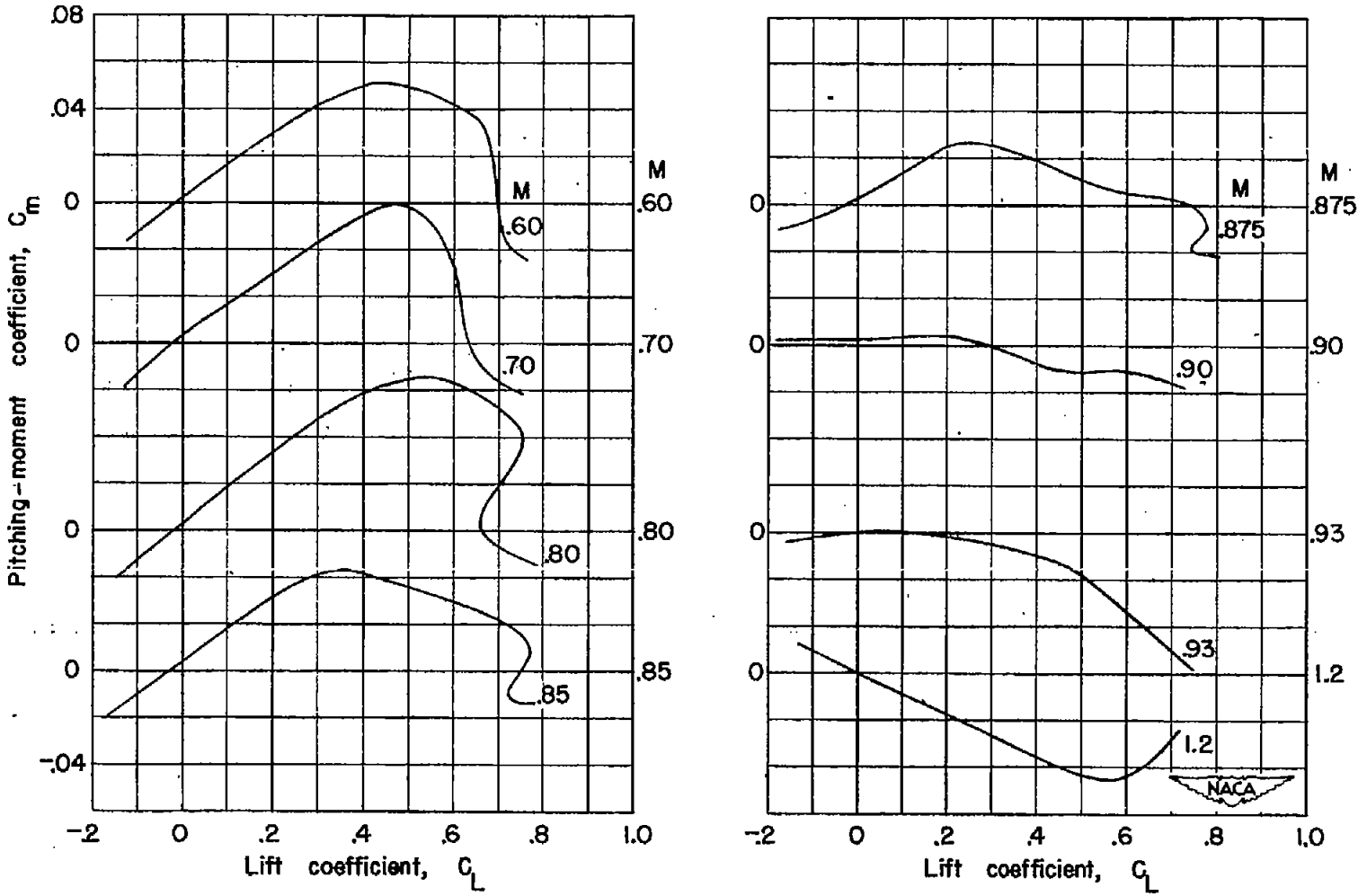

(c) Pitching-moment coefficient.

Figure 10.- Concluded.

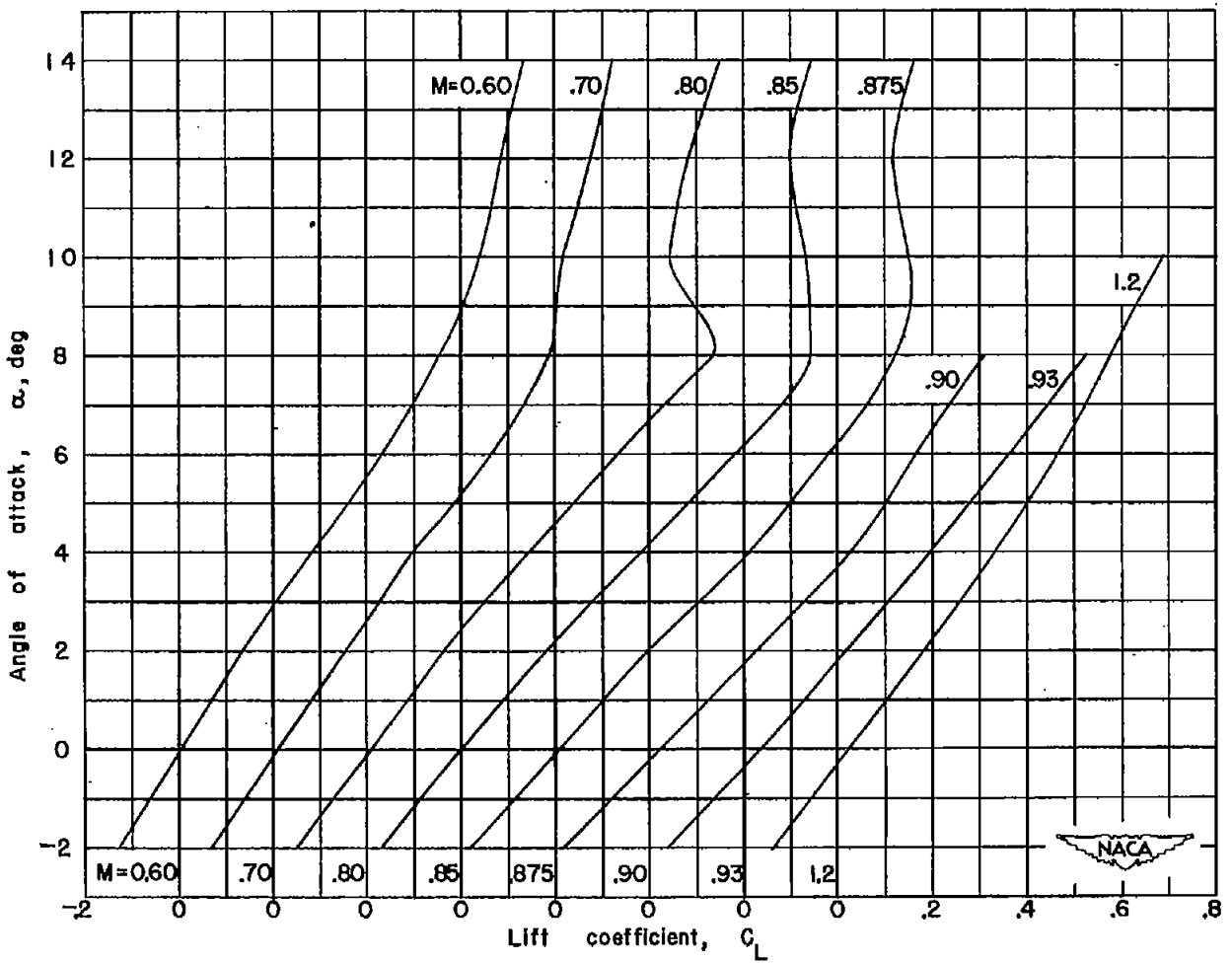

(a) Angle of attack.

Figure 11.- Variation of the aerodynamic coefficients with lift coefficient for the wing with wing-fuselage interference configuration.

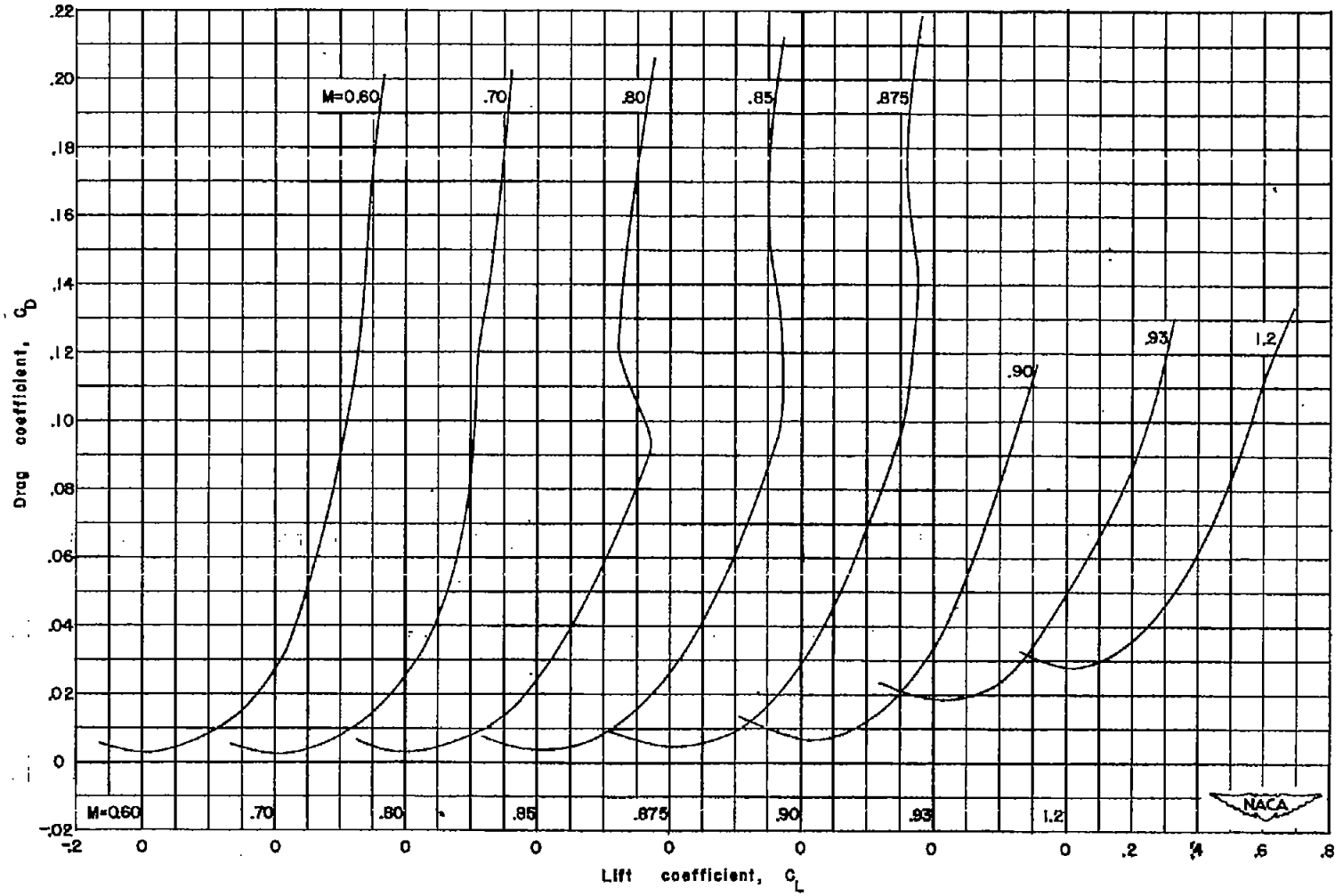

(b) Drag coefficient.

Figure 11.- Continued.

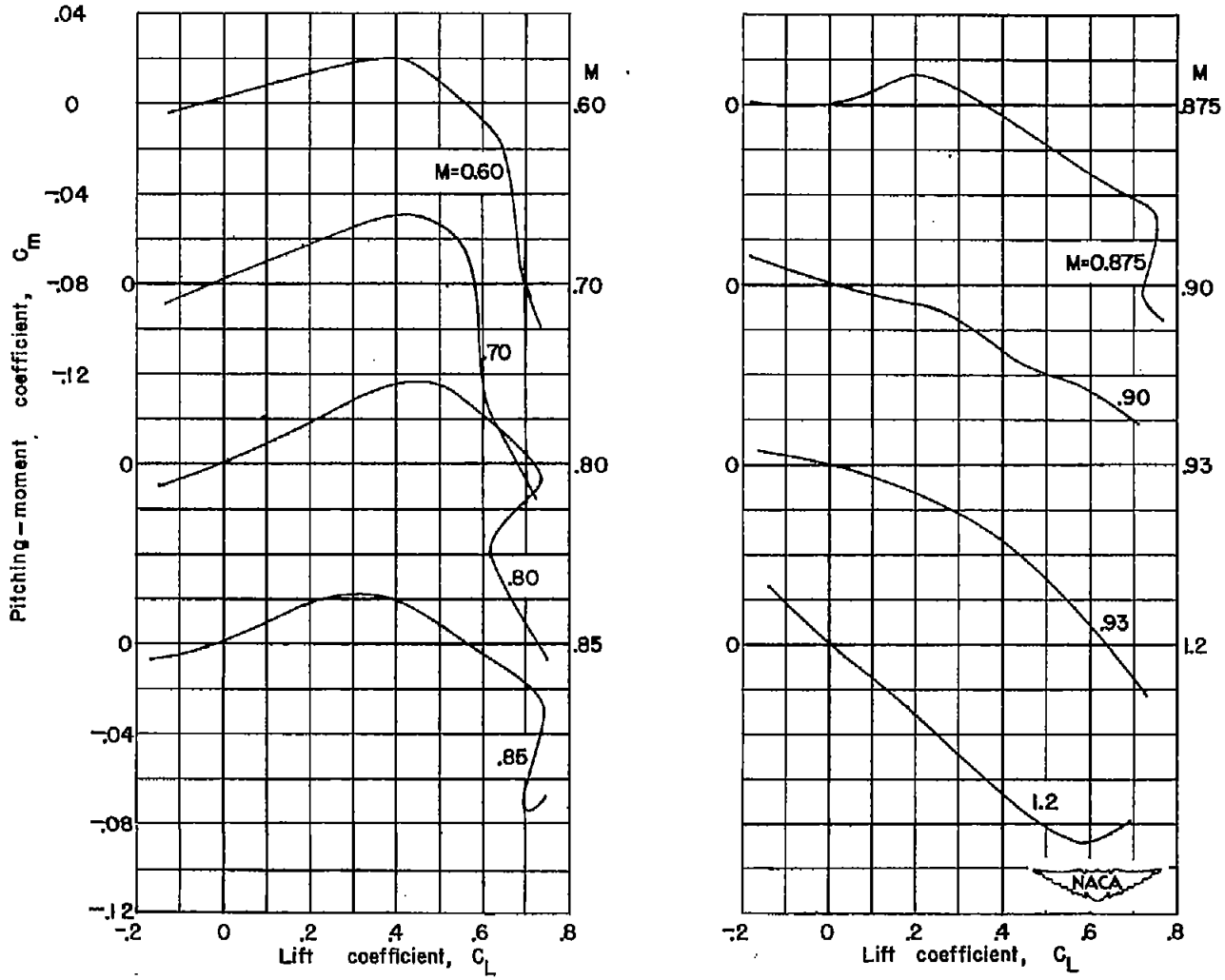

(c) Pitching-moment coefficient.

Figure 11.- Concluded.

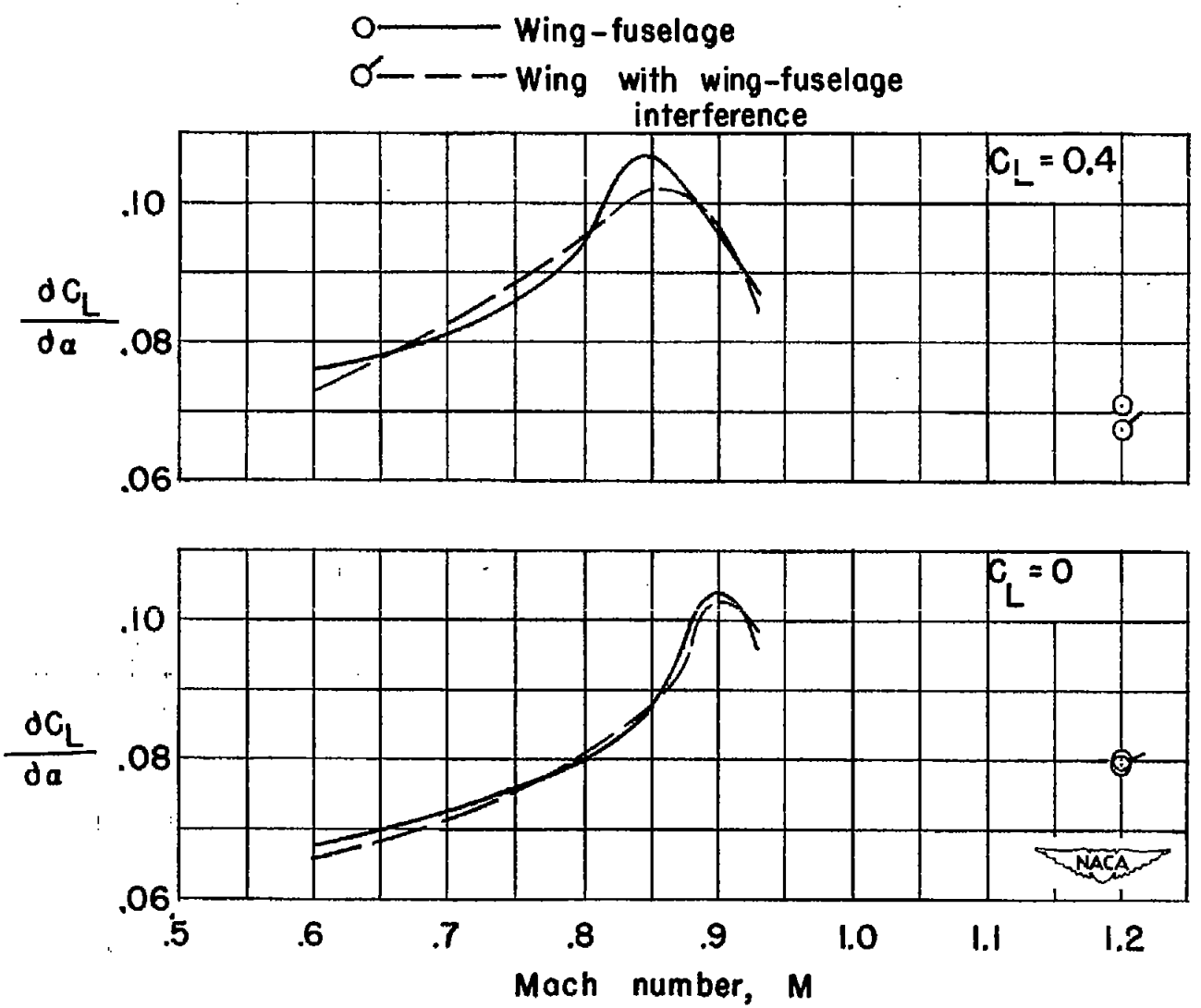

Figure 12.- Lift-curve-slope variation with Mach number.

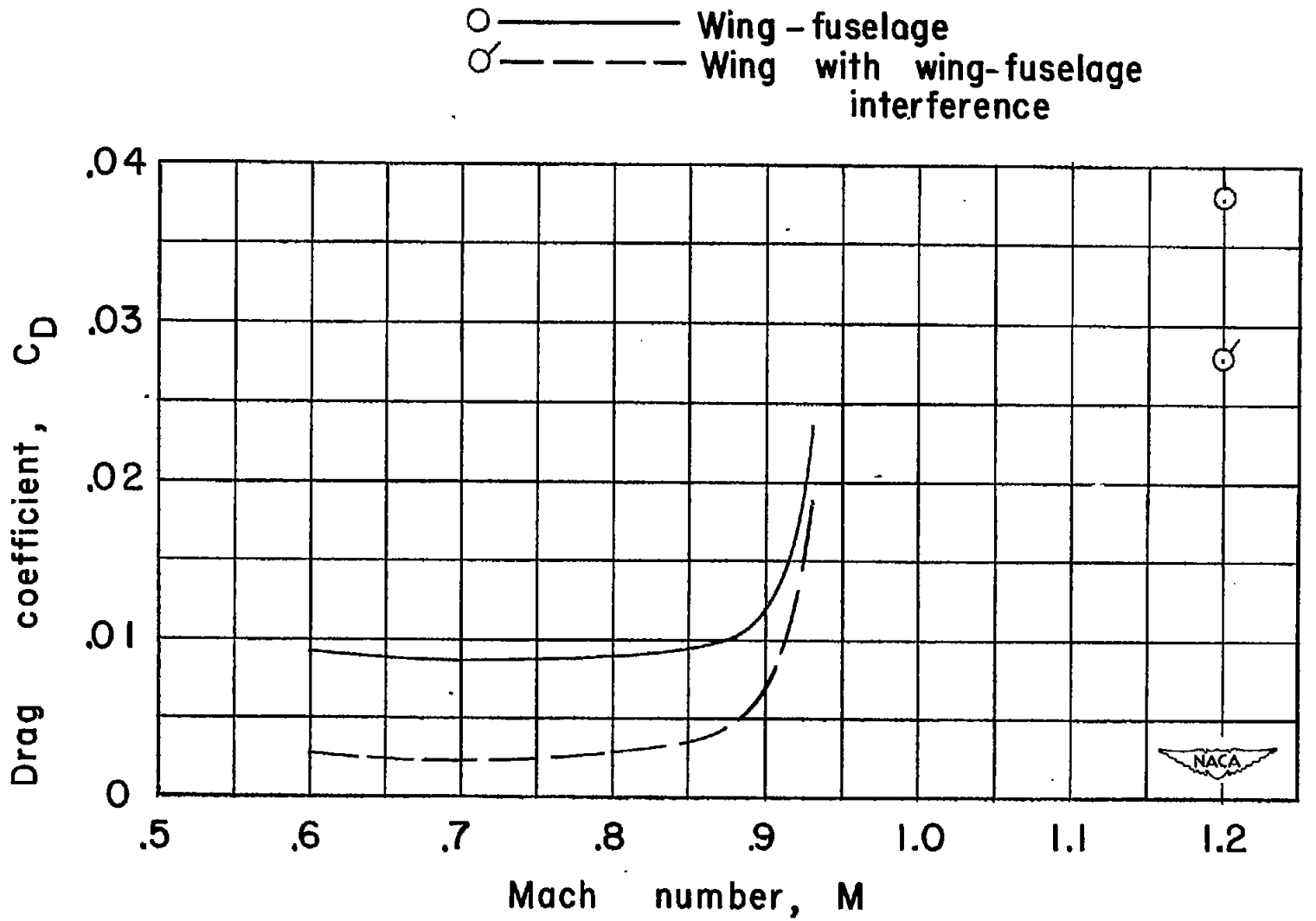

Figure 13.- Drag coefficient at zero lift coefficient variation with Mach number, corrected for sting interference.

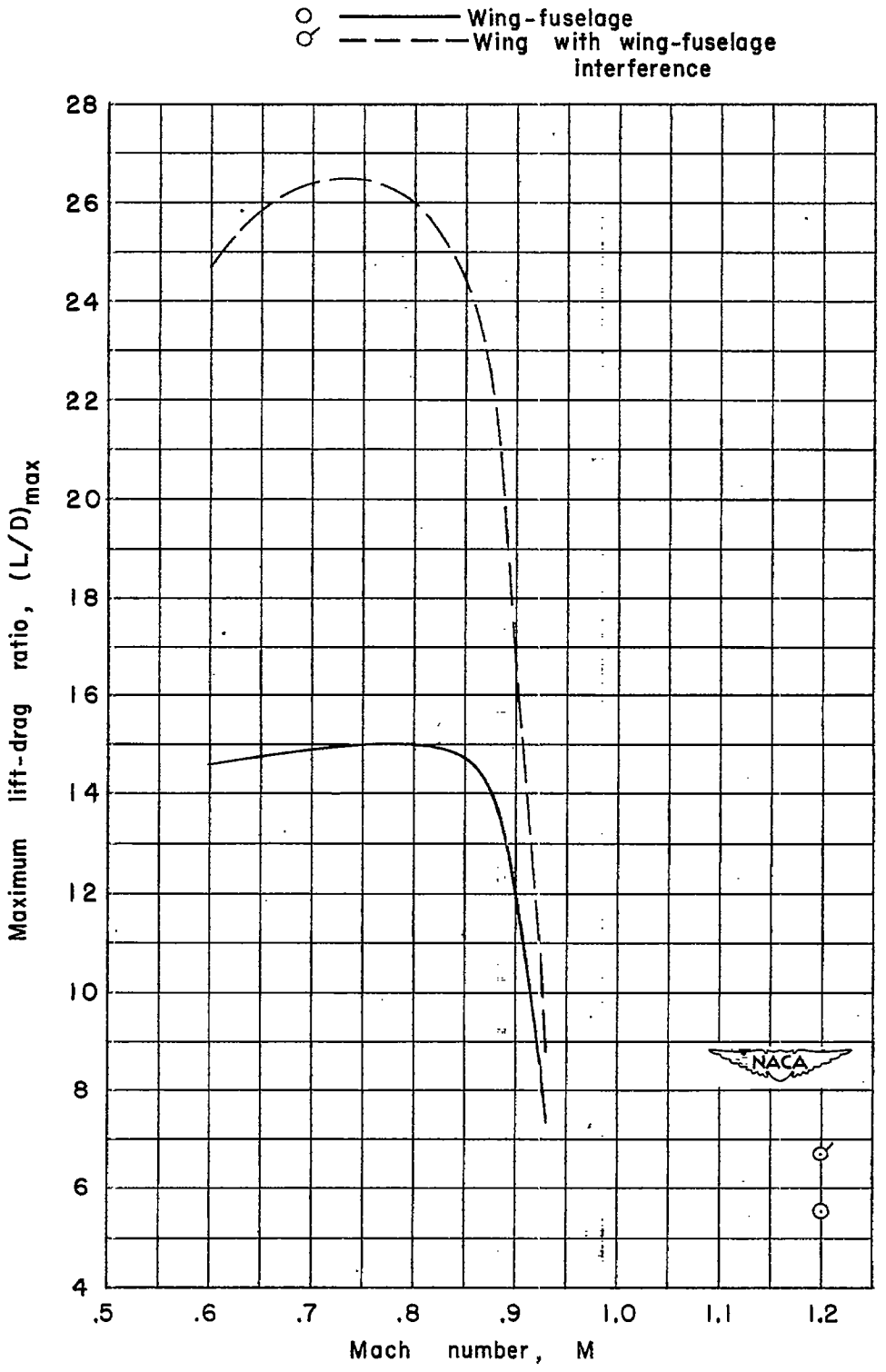

Figure 14.- Maximum lift-drag ratio variation with Mach number, corrected for sting interference.

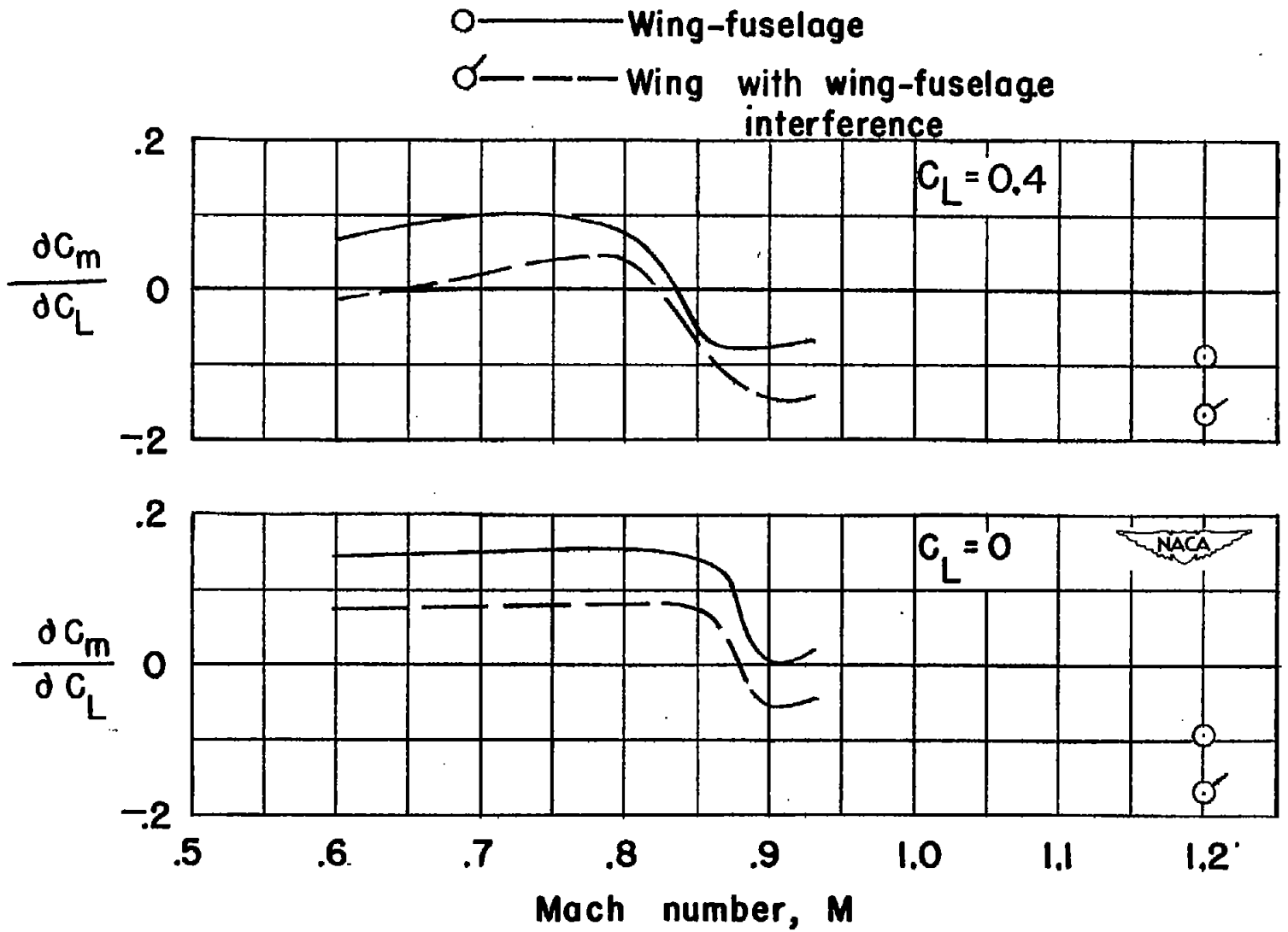

Figure 15.- Static-longitudinal stability-parameter variation with Mach number.

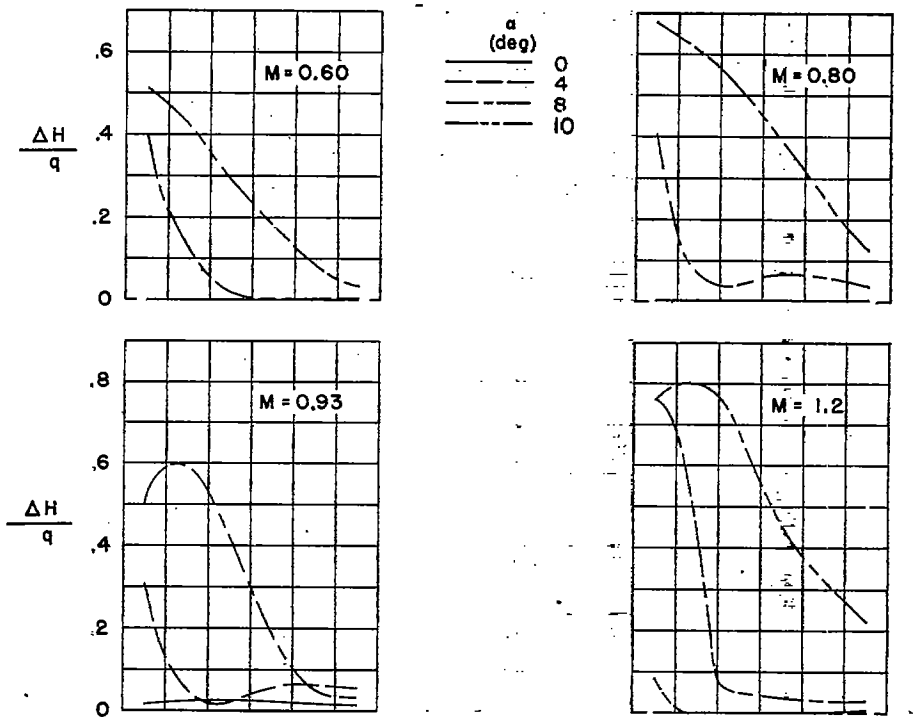

(a) Location 0.083 semispan from plane of symmetry.

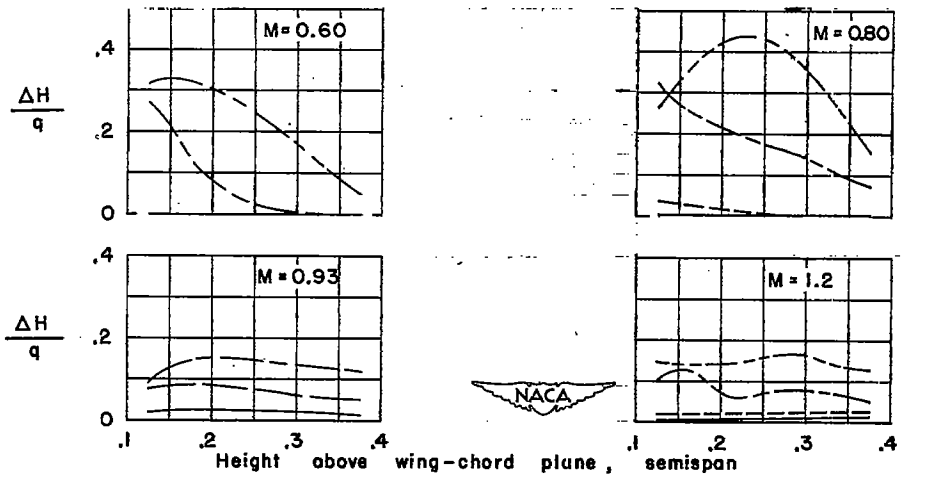

(b) Location 0.292 semispan from plane of symmetry.

Figure 16.- Wake losses 1.225 semispans behind the 0.25$\bar{c}$ location for the wing-fuselage configurations.

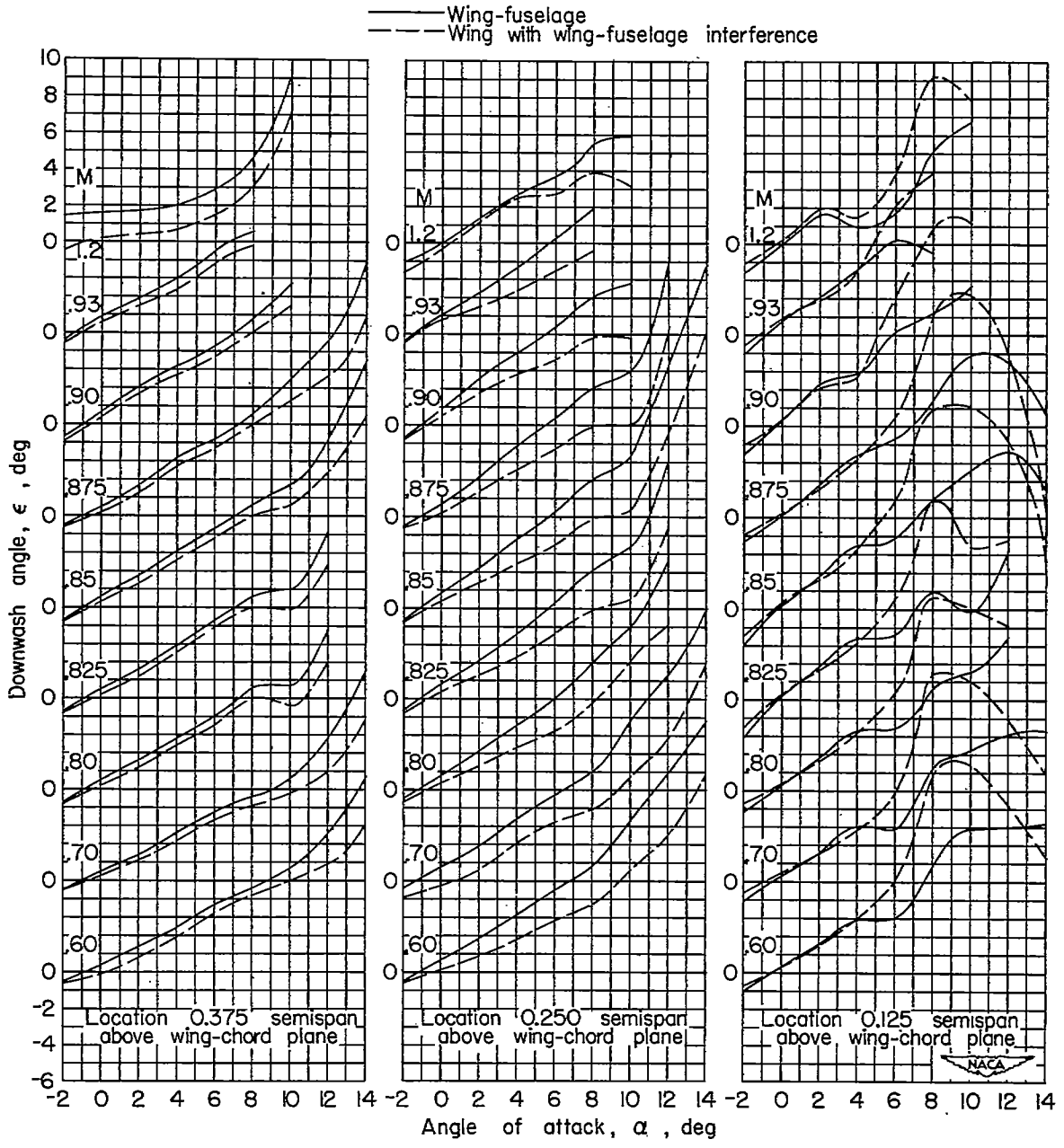

(a) Location 0.083 semispan from plane of symmetry.

Figure 17.- Variation of downwash 1.225 semispans behind the 0.25$\bar{c}$ location with angle of attack for the wing-fuselage and the wing with wing-fuselage-interference configurations.

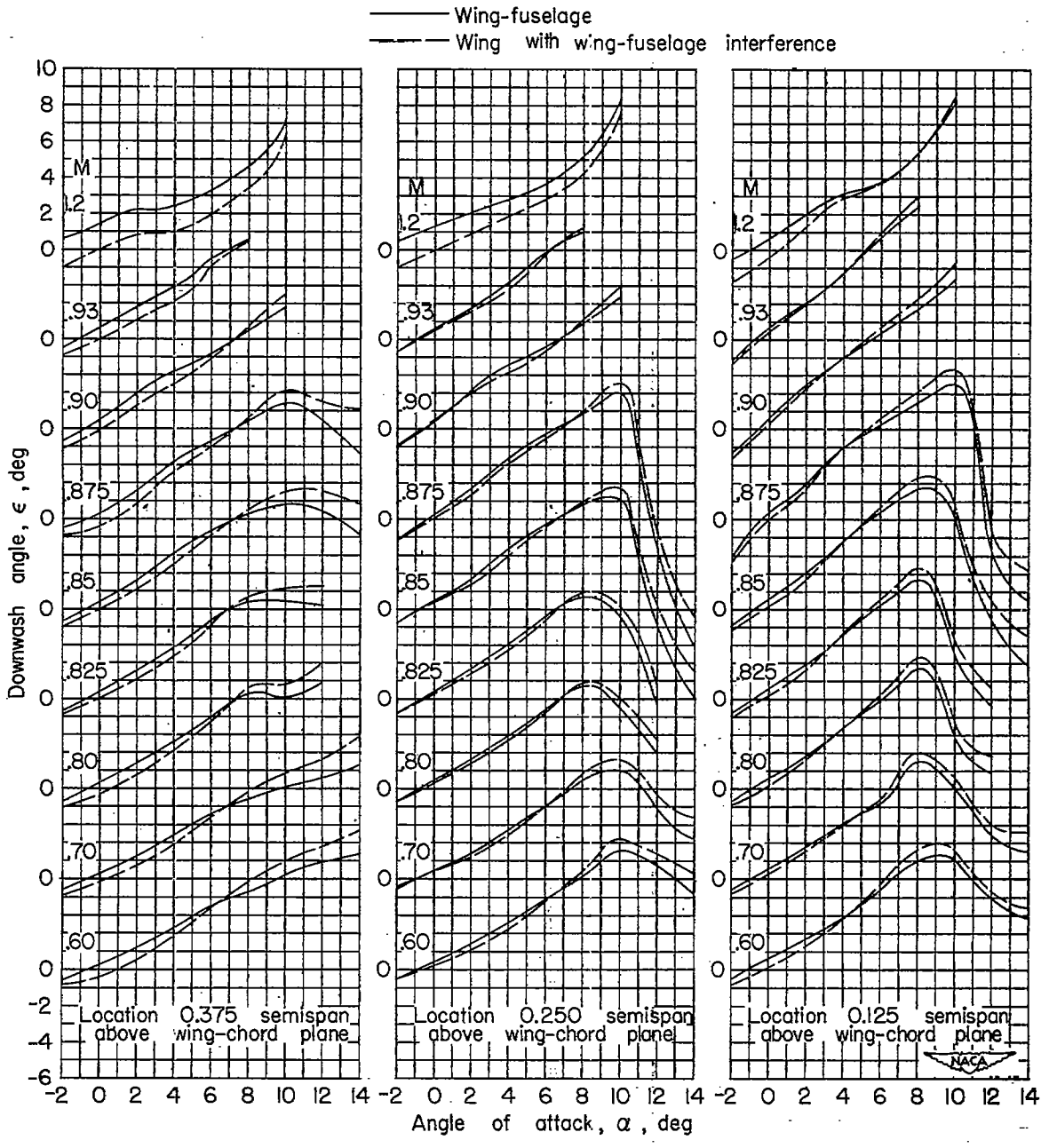

(b) Location 0.292 semispan from plane of symmetry.

Figure 17.- Concluded.

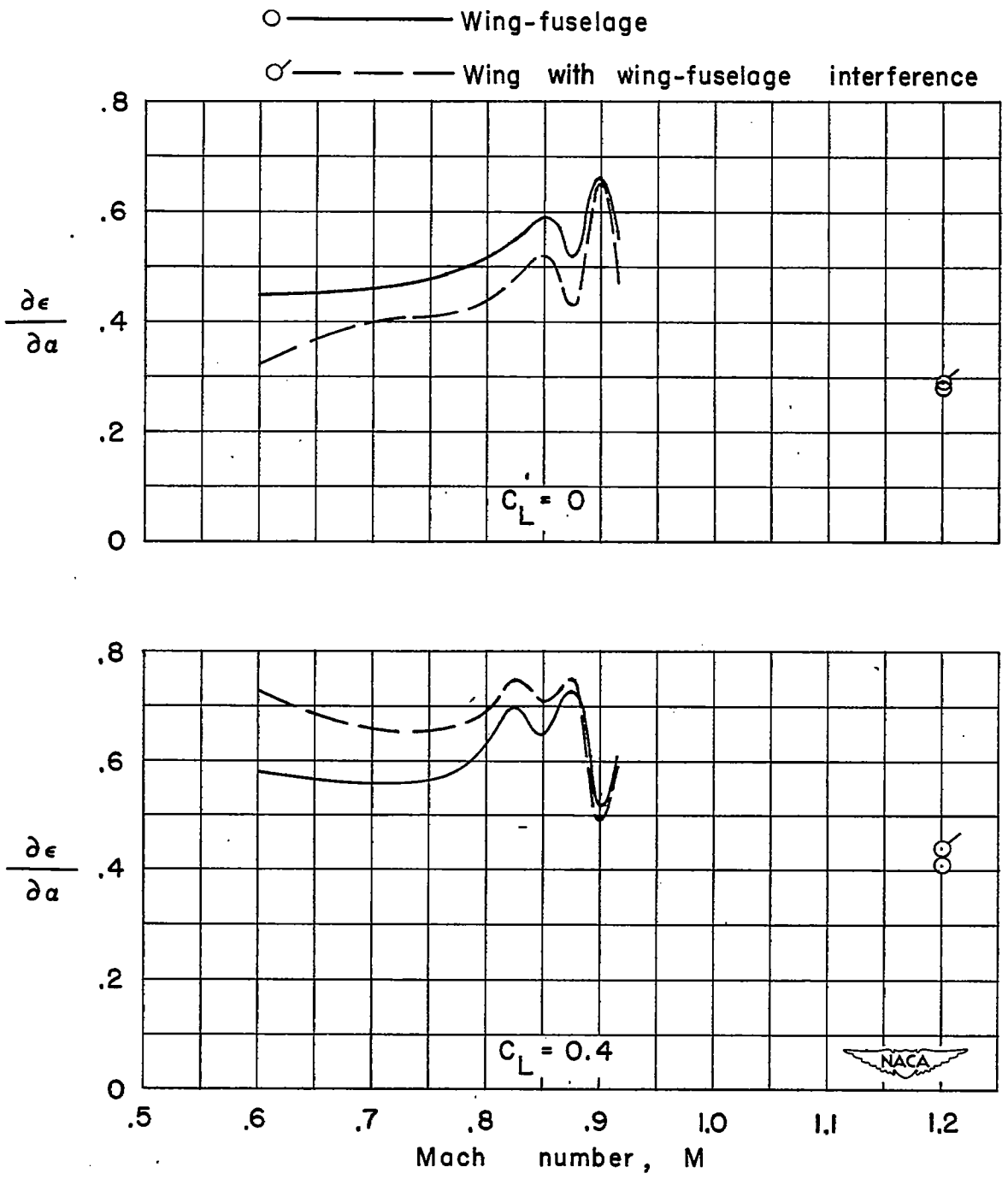

Figure 18.- Variation with Mach number of the average rate of change of downwash angle with angle of attack for a location 0.375 semispan above the wing-chord plane and 1.225 semispans behind the 0.25$\bar{c}$ position for the wing-fuselage with the wing and wing-fuselage-interference configurations.

NACA-Langley - 3-6-51 - 325